TITLE:

Mobile PEAR transcription factors integrate hormone and miRNA cues to prime cambial growth

AUTHORS:

Shunsuke Miyashima[2,3]*, Pawel Roszak[1,2]*, Iris Sevilem[2]*, Koichi Toyokura[1,7], Bernhard Blob[1]**, Jung-ok Heo[1,2], Nathan Mellor[8], Hanna Help-Rinta-Rahko[2], Sofia Otero[1], Wouter Smet[4,5,6], Mark Boekschoten[6], Guido Hooiveld[6], Kayo Hashimoto[3,9], Eva-Sophie Wallner[12], Yuki Kondo[10], Charles Melnyk[11], Thomas Greb[12], Keiji Nakajima[3], Ross Sozzani[13], Anthony Bishopp[8], Bert De Rybel[4, 5, 6 #], Ykä Helariutta[1, 2 #]**

AFFILIATION:

1: The Sainsbury Laboratory, University of Cambridge, Cambridge, CB2 1LR, UK

2: Institute of Biotechnology, Department of Biological and Environmental Sciences, University of Helsinki, FIN-00014, Finland

3: Graduate School of Sciences and Technology, Nara Institute of Science and Technology, Nara, 630-0192 Japan

4: Ghent University, Department of Plant Biotechnology and Bioinformatics, 9052 Ghent, Belgium

5: VIB Center for Plant Systems Biology, 9052 Ghent, Belgium

6: Wageningen University, Laboratory of Biochemistry, 6708 WE, Wageningen, The Netherlands

7: Department of Biological Sciences, Graduate School of Science, Osaka University, Toyonaka, Osaka, 560-0043, Japan

8: Centre for Plant Integrative Biology (CPIB) and School of Biosciences, University of Nottingham, Nottingham, LE12 5RD, UK

9: Graduate School of Humanities and Sciences, Nara Women's University, Nara, 630-8506 Japan

10: Department of Biological Sciences, Graduate School of Science, The University of Tokyo, Tokyo, 113-0033, Japan

11: Department of Plant Biology, Swedish University of Agricultural Sciences, 756 51 Uppsala, Sweden

12: Centre for Organismal Studies (COS), Heidelberg University, 69120 Heidelberg, Germany

13: Department of Plant and Microbial Biology, North Carolina State University, Raleigh, NC 27695, United States.

Corresponding author. Email: Ykä Helariutta: yrjo.helariutta@slcu.cam.ac.uk; Bert De Rybel: beryb@psb.vib-ugent.be

* These authors contributed equally to this work.

** These authors contributed equally to this work.

While apical growth in plants initiates upon seed germination, radial growth is only primed during early ontogenesis in procambium cells and activated later by the vascular cambium[1]. Although it is not known how radial growth is organized and regulated in plants, this system resembles the developmental competence observed in some animal systems, in which pre-existing patterns of developmental potential are established early on[2-4]. Here we show that the initiation of radial growth occurs around early protophloem sieve element (PSE) cell files of the root procambial tissue in Arabidopsis. In this domain cytokinin signalling promotes expression of a pair of novel mobile transcription factors, PHLOEM EARLY DOF (PEAR1, PEAR2) and their four homologs (OBP2, DOF6, TMO6 and HCA2), collectively called PEAR proteins. The PEAR proteins form a short-range concentration gradient peaking at PSE and activating gene expression that promotes radial growth. The expression and function of PEAR proteins are antagonized by well-established polarity transcription factors, HD-ZIP III[5], whose expression is concentrated in the more internal domain of radially non-dividing procambial cells by the function of auxin and mobile miR165/166. The PEAR proteins locally promote transcription of their inhibitory HD-ZIP III genes, thereby establishing a negative feedback loop that forms a robust boundary demarking the zone of cell divisions. Taken together, we have established a network, in which the PEAR - HD-ZIP III module integrates spatial information of the hormonal domains and miRNA gradients during root procambial development, to provide adjacent zones of dividing and more quiescent cells as a pre-pattern for further radial growth.

Cambial growth in plants is initiated within the procambial tissues of the apical meristems through periclinal (i.e. longitudinal) divisions associated with formation of the vascular tissues xylem and phloem[1] (Extended Data Fig. 1a). It has been established that during procambial development in Arabidopsis roots there are distinct domains for high auxin and cytokinin signalling, which mark the regions for further development of xylem and phloem/procambium, respectively[6-9]. To accurately map the spatial distribution of the periclinal divisions, we established a new nomenclature for the root procambial cells, including PSE-lateral neighbors (PSE-LN), as cells directly contacting both PSE and the pericycle, the outer procambial cell (OPC), as a procambial cell adjacent to the pericycle but not contacting PSE, and SE-internal neighbor (PSE-IN) as cells located internal to and directly contacting PSE (Fig. 1a). Both the PSE cell and PSE-LN showed higher activity of periclinal cell division than the OPC and PSE-IN (Fig. 1b, Extended Data Fig. 1b-d and Supplementary Information). We observed virtually no periclinal divisions in metaxylem (MX) and internal procambial cell (IPC) (Fig. 1b). Furthermore, blocking symplastic transport genetically[10] between the PSE and the surrounding cells results in a dramatic reduction in the number of cell files, not only in PSE lineage but also in the PSE-LN lineage (Extended Data Fig. 2a-e). Thus, the proliferative activity in procambium is centered on and around PSE and may involve symplastic intercellular signals.

By searching for transcription factors enriched in early PSE[11] (Extended Data Fig. 3a), we identified a pair of DOF transcription factors[12], *PHLOEM-EARLY-DOF 1* (*PEAR1)/DOF2.4* and

PEAR2/DOF5.1, that when overexpressed, increase the cell file number in vascular tissues (Extended Data Fig. 3b and c). Both RNA *in situ* hybridization and transcriptional fusion constructs revealed that *PEAR1* and *PEAR2* are expressed specifically in PSE cells (Fig. 1c-f). However, fluorescent tagged versions of both PEAR proteins show localization not only in PSE but also in PSE neighboring cells (PSE-LN and PSE-IN), indicating that these proteins move across short ranges via plasmodesmata (Fig. 1g-h, Extended Data Fig. 2f-g and 4a-d). Both *pear1* and *pear2* single and *pear1 pear2* double loss-of-function mutants displayed a small but significant reduction in vascular cell number (Fig. 2a, b, e and Extended Data Fig. 5a-c), but not to the extent seen when symplastic transport is blocked, suggesting additional functional redundancy.

[pear1 pear2 double no phenotype, we found OBP2 in same clade, expression in specific to PSE, make triple pear1 pear2 obp2, but no phenotype, quint from PEAR1 (only for Response letter and SI), again no phenotype]. [Compensation here, found another clade]. Consequently, we identified four additional PEAR homologs that show PSE-specific/abundant transcription pattern with broader protein localization, *DOF3.2/DOF6*[13], *DOF1.1/OBP2*[14], *DOF5.6/HCA2*[15], and *DOF5.3/TMO6*[16] (Extended Data Fig. 3d and e). Overexpression of *PEAR1*, *PEAR2*, or any of the four homologs resulted in an increased number of cell files (Extended Data Fig. 3c). [Mutant combination triple quad.] Combining up to five mutants to create the *pear1 pear2 dof6 obp2 hca2* line resulted in a population of slowly elongating roots (around 30 per cent, n=300) with further reduced radial growth (Fig. 2c, e and Extended Data Fig. 5a-c). The *pear1 pear2 dof6 obp2 hca2 tmo6* hextuple mutant resulted in all plants displaying a phenotype similar or more extreme to the strongest *pear* quintuple mutant [Complementation]. (Fig. 2d, e and Extended Data Fig. 5, and see Supplementary Information). Collectively these data indicate that the mobile PEAR proteins redundantly control cell proliferation in and around PSE cells. Their effects are likely to be both cell autonomous and/or non-cell autonomous as several putatively direct target genes, including a central regulator of phloem formation *SUPPRESSOR OF MAX2 1-LIKE3* (SMXL3)[17], are expressed in both PSE and its surrounding cells (Fig. 2f-i and Extended Data Fig. 6). Moreover, ectopic expression of SMXL3 is sufficient to enhance periclinal cell division (Fig. 2j-l).

Earlier studies have highlighted cytokinins in regulating procambial cell proliferation[7,9]. During root development, the cytokinin signalling reporter, *pARR5::RFPer*[8] partially overlaps with the PEAR transcriptional domain (Fig. 3b) and is initially activated and maintained in PSE and its surrounding procambial cells, later becoming concentrated in the procambial cells neighboring to the xylem cells[8,9] (Fig. 3a and b). Exogenous cytokinin application rapidly increased the level of *PEAR* transcripts (Extended Data Fig. 7a), and sustained cytokinin treatment resulted in radial expansion of *PEAR* expression domains (Extended Data Fig. 7b). Conversely, both *PEAR1* and *TMO6* transcription was absent in the vascular tissue of cytokinin signalling loss-of-function mutant *wooden-leg* (*wol*)[6,18] (Fig. 3c and Extended Data Fig. 7c) and in lines over-expressing ARR22[19], an inhibitor of cytokinin signalling (Fig. 3e and f). However, expression of both genes was restored by the induction of cytokinin signalling in *wol* (Fig. 3d and Extended Data Fig. 7d). Collectively this indicates that cytokinin

signalling promotes the transcription of *PEAR* genes in roots. During embryogenesis, high cytokinin response is initiated in vascular cells of upper lower tier (ult) at the early heart stage (Fig. 3g, h and Extended Data Fig. 7e, f), and only at the late heart stage is the characteristic bisymmetric pattern of cytokinin output established (Extended Data Fig. 7g-h). *PEAR1* transcription pattern was highly correlated with cytokinin signalling during embryogenesis, except for its broad expression in the early globular stage (Fig. 3k-l and Extended Data Fig. 7m-o). By contrast, in *wol* embryos, where no cytokinin response was detected within vascular cells (Fig.3i-j), *PEAR1* transcription was initially observed in the globular *wol* embryo (Fig. 3m), but was gradually attenuated after heart stage (Fig. 3n and Extended Data Fig.7p-r). Taken together our results indicate that during early embryogenesis initiation of *PEAR1* expression is independent of cytokinin signalling, but by the time the bisymmetric cytokinin pattern is formed at early heart stage, *PEAR1* transcription is activated and maintained post-embryonically by cytokinins.

Almost no periclinal cell divisions were observed in the cells non-adjacent to pericycle, including PSE-IN where both cytokinin response and PEAR protein are present (Fig. 1b-h and 3a-b), suggesting an inhibitory mechanism that restricts PEAR function in the inner cells. We previously observed increased cell number in the vascular tissue of quadruple loss-of-function mutant of the five *Class III HOMEODOMAIN LEUCINE ZIPPER (HD-ZIP III)* genes[20,21] (Fig. 4a, d and g). These ectopic cell divisions occur in cells non-adjacent to the pericycle (Fig. 4h, i and Extended Data Fig. 8a-c). We observed high levels of three HD-ZIP III proteins, PHABULOSA (PHB), CORONA (CNA) and REVOLUTA (REV), in non-dividing procambial cells, IPC and PSE-IN, whereas their expression was absent in the actively dividing cells of the PSE and PSE-LN (Fig. 4j and Extended Data Fig. 8d-h). In this domain endodermal-derived mobile miR165/6 eliminates *HD-ZIP III* messenger RNA [21,22], suggesting that HD-ZIP III inhibit periclinal cell divisions of PSE-IN by antagonizing the functions of co-localized PEAR proteins. This is further supported by our observation that overexpression of *PEAR1* in the miRNA-resistant *phb-1d* mutant which has elevated levels of PHB[21,22] is less effective than overexpressing PEAR1 in wild-type plants (Extended Data Fig. 8i-l). Hence, in order to sharpen the boundary between dividing and non-dividing cells, the expression pattern of both HD-ZIP III and PEAR proteins has to be tightly controlled.

Auxin is known to promote the xylem associated *HD-ZIP III* transcription[23,24]. However, *PHB*, *CNA* and *REV* show broader expression of both transcriptional and translational reporters (Fig. 4j, k, Extended Data Fig. 8d, e, g, h and Extended Data Fig. 9), suggesting that other factors may enhance *HD-ZIP III* transcription in the peripheral region. Interestingly, we observed significant reduction of *CNA* transcription in PSE-neighboring cells in the *pear* quintuple background (Fig. 4k-m). In addition, *PEAR1* overexpression enhanced the transcription of *HD-ZIP III* genes, especially in the central domain of vascular tissue (Extended Data Fig. 9). These data suggest that PEAR locally enhance *HD-ZIP III* transcription at PSE-neighboring cells. As previous work has reported that PEAR1 has the potential to bind *HD-ZIP III* promoters[25,26], it is possible that these interactions are direct. As *HD-ZIP III* and *PEAR1* show complementary expression patterns, we explored whether HD-ZIP III could

regulate *PEAR1* transcription. *PEAR1* expression was severely attenuated in mutants showing elevated levels of HD-ZIP III such as *phb-1d* and *shr-2*[21] (Extended Data Fig.8m-q). Together these data suggest a feedback loop between HD-ZIP III and PEAR1 transcription.

Furthermore, to examine a possible effect of the HD-ZIP III on the mobile PEAR1 proteins, we measured the diffusion coefficient and movement pattern of PEAR1-GFP in wild type and in the *hd-zip III* quadruple mutant where *PEAR1* was transcribed at PSE with a triarch arrangement (Extended Data Fig. 8r and s). We observed that the diffusion coefficient of PEAR1-GFP is significantly higher and the protein moves further in the mutant compared to wild type (Fig. 4n-p and Extended Data Fig. 4). To understand the significance of this enhanced PEAR1 movement, we analyzed the cell proliferation pattern of combinatorial *pear1 pear2 obp2 dof6 hca2 phb phv cna athb*8 nonuple and *pear1 pear2 obp2 dof6 hca2 tmo6 phb phv cna athb8* decuple loss-of-function mutants. We found that these mutants showed reduced number of periclinal cell divisions in the vascular cells both adjacent to and non-adjacent to the pericycle (Fig. 4a-i). This indicates that HD-ZIP III inhibits the periclinal cell division partially through inhibiting PEAR1 movement to position the cell division zone around phloem. In order to further conceptualize the observed interactions between PEAR and HD ZIP III, we incorporated the PEAR genes into a network model with HD-ZIP III, miR165/6, auxin and cytokinin as defined in previous theoretical studies [9,27,28] (Supplementary Modelling Information). The network includes a negative feedback loop, in which HD-ZIP III transcription is activated by PEAR1 (Interaction (1) in Fig.4q), in turn PEAR1 transcription and protein movement is inhibited by HD-ZIP III (Interaction (2) and (3), respectively in Fig. 4q), The model is defined as a line in one spatial dimension representing 3, 4 or 5 cells from the center of the xylem axis to the outer edge of the PSE cell (Extended Data Fig. 10 and Supplementary Modelling Information). We ran simulations exploring the steady state patterns created in networks with the above interactions and in scenarios when one of the interactions was missing. The version of the model incorporating of all three interactions results in the sharpest gradients of PEAR and HD-ZIP III proteins (Fig. 4r-t) with both PEAR1 protein and HD-ZIP III localized within the PS-IN, consistent with experimental observations (Extended Data Fig. 10a).

Collectively our research has uncovered a regulatory network, in which the spatial distribution of phytohormones and small RNA is decoded into the activity of two functionally antagonistic sets of transcription factors: PEAR and HD-ZIP III during root procambial development (Fig. 4u). In this module the well-established HD-ZIP III tissue polarity factors regulate protein movement. Within the root meristem, the mobile PEAR factors promote cell proliferation around the two early protophloem sieve element cell files, which constitute two new organizers just proximal to the quiescent center. These organizers surround a more quiescent central zone defined by the HD-ZIP III factors. In this way, the PEAR - HD-ZIP III module specifies a lateral meristem within an apical meristem and as such, forms a template for further cambial development[29]. Therefore, in the future it will be interesting to determine how extensively this procambial pathway also contributes to ontogenetically late processes such as wood and storage organ formation in the crop species.

Methods

Plant materials and growth condition.

Arabidopsis thaliana lines used in this study were either in Columbia or Landsberg erecta background. The following alleles were obtained from the publicly available collections: *pear1* (CSHL_GT8483) in Ler, *pear2* (SALK_088165) in Col-0, *obp2* (SK24984) in Col-4, *dof6* (Wiscseq_Ds_Llox351c08) in Col-0, *hca2* (GK-466B10) in Col-0. Knock-out alleles of TMO6 were generated using CRISPR-Cas9 technology as previously described[30]. The following protospacer target sequence was selected as it had no predicted off-site targets and allowed screening via *Nhe*I restriction using the CRISPR-P web tool[31]. The Protospacer adjacent motif is underlined: GGACACCTGAGAGCTAGCTCCGG. Successful mutagenesis was confirmed via Sanger sequencing in plants of the T2 and T3 generation that no longer carried the Cas9 transgene. Four TMO6 mutant alleles were identified: *tmo6-1* (+A), *tmo6-2* (+T), *tmo6-3* (deletion of 5 bp and at the same time insertion of 26 bp) and *tmo6-4* (-5 bp) (Extended Data Fig. 5a). The alleles *tmo6-1*, *-2*, and *-3* were found in the *pear* hextuple mutant and caused the *pear* hextuple phenotype, while *tmo6-4* was found in the *tmo6* single mutant, respectively. The genotyping primers for these mutants are listed in Supplementary Table 1. *hd-zip III* quadruple *(phb phv cna athb8*) was described previously[20]. Plant growth conditions were described previously[6].

Histological analysis

Primary roots of vertically grown 4 to 5-day-old seedlings were used for histological analyses. For confocal imaging, root samples were stained with propidium iodide (PI), aniline blue (AB) or SCRI Renaissance 2200 (SR2200) (Renaissance Chemicals, UK). The method of PI and AB staining were described previously[10,32]. For SR2200 stain, root samples were fixed in SR2200 solution (4% paraformaldehyde, 0.1% (v/v) SR2200 in PBS buffer (pH7.4)). Then samples were washed with PBS buffer and transferred into the ClearSee solution[33]. Confocal imaging was performed on Leica TCS SP5, Leica TCS SP8, Leica TCS SP5 II HCS-A or Nikon C2 CLSM using a solid state blue laser (480nm) for GFP, a green laser (514nm) for VENUS, a lime laser (DPSS 561nm) for RFP and PI, and a UV laser (diode 405nm) for SR2200. Transverse plastic sections of root were performed as described previously[6]. For histological analyses of embryo, dissected embryos were mounted in SR2200 solution and visualized by the confocal microscopy.

DNA Constructs and transgenic plants

Most of transgenic constructs were produced by using Gateway or multisite Gateway system (Invitrogen) as described previously[34]. To generate the transcriptional fusion constructs with GFP-GUS each promoter sequence was cloned into pDONR221 and fused to GFP-GUS coding sequence in the destination vector pBGWFS7 by normal LR reaction. For other transcriptional fusion constructs, including *pPEAR1::VENUSer*, *pPEAR2::VENUSer*, *pAHA3::RFPer*, *pOBP2::VENUSer*, *pHCA2::RFPer*, *pTMO6::RFPer* and *pREV::RFPer* and the transcriptional fusion constructs of

PEAR1/PEAR2 downstream genes, each promoter was cloned into pDONRP4_P1R, and assembled with the coding sequence of fluorescent reporter (VENUSer or RFPer) and terminator into the destination vectors, pHm43GW (Hygromycin resistant), pBm43GW (Basta resistant) or by multisite Gateway system. To produce the transcriptional fusion constructs of HD-ZIP III, including PHB and CNA, each promoter was inserted upstream of the GAL4:VP16 (GV) coding region of pBIB-UAS-GFPer-NtADH5'-GV vector[35]. For most of the translational fusion constructs of PEAR genes, except for pPEAR1::PEAR1-GFP, each promoter was cloned into the first-box vector pDONRP4_P1R, and each coding sequence was cloned into vector pDONR221, thereafter each promoter and coding sequence were assembled with pDONR P2R_P3-terminator/reporter into pHm43GW, pBm43GW or pFR7mGW by multisite Gateway system[34]. To generate other translational fusion constructs, including *pPEAR1::PEAR1-GFP*, *pCNA::CNA-GFP*, *pATHB8::ATHB-GFP* and *pREV::REV-GFP*, each genomic fragment which contains promoter, coding and its 3' region, was cloned into pAN19 vector. Then GFP coding sequence was fused to C-terminus of each coding sequence. Finally, each translational fusion sequence was inserted into the modified pBIN19 vector with Basta resistance[22]. For the overexpression construct, including *PEAR* genes and *CRE1*, the coding sequence of each genes was assembled with stele-specific estradiol-inducible promoter (pCRE1[XVE]) into pHm43GW or pBm43GW by the Multisite Gateway system described previously[34]. To construct *pPEAR1[XVE]::icals3m*, 1.5kb *PEAR1* promoter was cloned into p1R4-ML:XVE vector, and assembled with icals3m sequence into pBm43GW[10]. The primers for DNA construction and the list of plasmids are shown in Supplementary Table 1 and 2.

In situ hybridization

Amplified fragments of *PEAR1*, *PEAR2* and *OBP2* were cloned into pGEM-T Easy (Promega) vector and fragments of *DOF6*, *HCA2*, *TMO6* into pCR-Bunt II-TOPO vector (Invitrogen) following manufacturer's instructions. In order to obtain antisense probes, plasmids were first linearized by restriction enzyme treatment: *Mlu*I for *PEAR1* and *OBP2*, *Sca*I for *PEAR2*, *Hind*III for *TMO6* and *DOF1*, and *Xba*I for *HCA2* were used. Linearized plasmids were digoxigenin (DIG) labelled using DIG RNA Labelling Kit (Roche) following manufacturer's instructions. For *PEAR1*, *OBP2*, *TMO6* and *DOF1*, T7 RNA polymerase and for *PEAR2* and *HCA2*, SP6 RNA polymerase were used. mRNA detection on a whole-mount seedlings was performed as described[36]. Images were taken with Zeiss Axioimager microscope with either 20x or 40x objective.

Transcriptome analysis

Targets of PEAR1 and PEAR2 were identified by analyzing transcriptional changes after dexamethasone (DEX) treatment of *pRPS5A::PEAR1-GR* and *pRPS5A::PEAR2-GR*. To identify putative direct targets, DEX treatment was also performed with cycloheximide (CHX), which inhibits protein synthesis and therefore activation of indirect targets. 3-day-old seedlings were grown on control medium and transferred to medium containing 10 μM DEX or 10 μM DEX and 10 μM CHX

for 2h, after which root tips were collected and RNA extraction was performed. Total RNA (100 ng) was labeled using GeneChip WT PLUS Reagent Kit (Thermo Fisher Scientific) and hybridized to GeneChip Arabidopsis Gene 1.1 ST array plates (Affymetrix). Sample labeling, hybridization to chips, and image scanning were performed according to the manufacturer's instructions. Microarray analysis was performed as previously described to yield significantly up-regulated genes (>1.0-fold; $P < 0.05$)[9]. Venn diagram of significantly up-regulated genes was made using Venny 2.1 on-line program (http://bioinfogp.cnb.csic.es/tools/venny_old/venny.php). Previously published root spatiotemporal expression data was used to make a heatmap to visualize predicted expression patterns of all PEAR1 and PEAR2 targets[11]. To have relative expression values for every gene in different root cell types and developmental stages, values for every gene were normalized based on its highest expression in one of the cell types. Heatmap was generated using R with gplots R-package[37]. The transcriptomics data files are submitted to GEO (accession number GSE115183).

Reporter analysis of PEAR1/2 downstream genes

When selecting genes for reporter analysis, putative direct targets were preferred. Significantly more direct targets were identified for *PEAR2*, and therefore those are overrepresented. Other considerations were how strongly they were upregulated, as well as their predicted expression pattern. Expression in early procambium or early phloem and procambium was preferred. *AT1G49230*, *AT1G15080*, *AT3G16330*, *AT4G00950* and *SMXL3* are putative direct targets of PEAR2 and with predicted expression in early phloem/procambium. *AT3G54780* was chosen because it is a putative direct target of both PEAR1 and PEAR2, although no predicted expression data was available. *AT1G09460* is a direct target of PEAR2 and target of PEAR1, and was chosen because it was induced very strongly by both genes, although predicted to be expressed only very weakly in phloem/procambium.

Quantitative RT-PCR Analysis

qRT-PCR analyses were performed as described previously[38]. Cytokinin treatment was done with 10μM 6-Benzylaminopurine (BA). RNA was extracted with the RNeasy kit (QIAGEN). Poly(dT) cDNA was prepared from 1 μg of total RNA with an iScript cDNA Synthesis Kit (Biorad) and analyzed on a CFX384 Real-Time PCR detection system (BioRad) with iQ SYBR Green Supermix (BioRad) according to the manufacturer's instructions. Expression levels were normalized to those of EEF1α and CDKA1;1. The primers are listed in Supplementary Table 1.

Phloem transport assay

The phloem translocation was judged by the transport and unloading of 5(6) carboxyfluorascein diacetate (CFDA) as describe[39]. After application of the dye, plants were kept in agar plates and only placed on regular cover slips for imaging.

Raster image correlation spectroscopy (RICS)

We applied RICS to determine the rate of movement of GFP-labeled PEAR1 protein in wild type and *hd-zip III* quadruple *(phb phv cna athb8*) mutant background. Signal was measured in vascular cells within the 70 μm distance from the QC. The SimFCS Software[40], was used to perform RICS analysis and to determine diffusion coefficient in both genetic backgrounds. Scanning of the samples was performed using following parameters: image size: 256x256 px, pixel size 100 nm, pixel dwell 8.19 μsec. Whole procedure was performed as described earlier[41].

Mathematical model

The mathematical model is formulated as a set of ordinary differential equations describing the set of interactions shown in Figure 4o, defined on a one-dimensional array of discrete spatial compartments representing a cross-section of root tissue. The spatial subdivisions may represent either cell or cell wall compartments, with multiple compartments per cell so that intracellular resolution is present within the model. Three, four or five cells are simulated, from the centre of the stele at the xylem axis to the edge of the stele where phloem is formed. The model is implemented as a single stand-alone text file using Python 2.7 plus the open source libraries Scipy, from which the 'odeint' function was used to solve the differential equations, and Matplotlib, which was used to plot the figures. See Supplementary Modelling Information for more details.

Code availability

The code for mathematical model is available on request.

Data availability

All lines and data supporting the findings of this study are available from the corresponding author upon request. The microarray data sets are available GEO (accession number GSE115183).

Acknowledgements

We thank E. Scarpella, A. P. Mähönen, ABRC and NASC for materials, Natalie Clark for assisting with the scanning FCS analysis, Jenny Jansen for technical assistance with microarray hybridizations, Oleg Kambur and Lothar Kalmbach for assistance in generating the heatmap, and D. Weijers for helpful discussions, A. Groenheide, E. Cornelissen, M. Chu, A. Korpoo and Alba Rodriguez Diez for technical support. This works was supported by Finnish Centre of Excellence in Molecular Biology of Primary Producers (Academy of Finland CoE program 2014-2019) decision #271832, the Gatsby Foundation [GAT3395/PR3)], University of Helsinki [award 799992091] and the European Research Council Advanced Investigator Grant SYMDEV [No. 323052] to Y. H., a NSF-BBSRC MCSB 1517058 to R.S. and Y.H., an ERC Consolidator grant (PLANTSTEMS), a Heisenberg Professorship of the German Research Foundation (DFG, GR2104/5-1) and the SFB 873 (DFG) to T.G., the Netherlands Organization for Scientific Research (NWO; VIDI-864.13.001) and The Research Foundation - Flanders (FWO; Odysseus II G0D0515N and 12D1815N) to W.S. and B.D.R.,

respectively, a JSPS postdoctoral fellowship for research abroad to S.M., Swiss National Science Foundation Postdoc Mobility Grant (P300P3_147894) to P.R., a JSPS Research Fellowship for Young Scientists and JSPS KAKENHI Grant [JP16J00131] to K.T., Bayer Science and Education Foundation, German Academic Exchange Service (DAAD) to B.B., The Finnish Academy of Science to J. O. H., Herchel Smith Postdoctoral Research Fellowship (Herchel Smith Fund) to S.O.

Author contributions

S.M., P.R. and I.S. contributed equally to this work. S.M. characterized the molecular interactions among PEAR and HD-ZIP III module. P.R. identified and quantified phenotype in the PEAR loss of function mutants with help of B.B. I.S. determined phloem specific DOF and their downstream genes with input from B.D.R., W.S., M.B. and G. H. K.T. characterized PEAR-HD-ZIP III combinatorial mutants. B.B. generated tmo6 CRISPR mutants. J.H. performed in situ hybridization. N.M. and A.B. designed and performed computational modelling. H.H. produced CRE1 inducible line. S.O. assisted in the microarray experiments. K.H. and K.N. produced HD-ZIP III reporter lines. E.S.W., Y.K., T.G. and C.M. shared informative non-published data. R.S. analyzed diffusion coefficient of PEAR1-GFP with P.R. B.D.R. and Y.H. participated in experimental design. S.M. and Y.H. wrote the manuscript and all authors commented on the manuscript. B.D.R. and Y.H. are co-corresponding authors.

Reference

1 Esau, K. *Vascular differentiation in plants*. (Holt, Rinehart and Winston, 1965).

2 Crick, F. H. & Lawrence, P. A. Compartments and polyclones in insect development. *Science* **189**, 340-347 (1975).

3 Reggiani, L., Raciti, D., Airik, R., Kispert, A. & Brändli, A. W. The prepattern transcription factor Irx3 directs nephron segment identity. *Genes Dev* **21**, 2358-2370, doi:10.1101/gad.450707 (2007).

4 Dickson, B., Sprenger, F. & Hafen, E. Prepattern in the developing Drosophila eye revealed by an activated torso--sevenless chimeric receptor. *Genes Dev* **6**, 2327-2339 (1992).

5 McConnell, J. R. *et al.* Role of PHABULOSA and PHAVOLUTA in determining radial patterning in shoots. *Nature* **411**, 709-713, doi:10.1038/35079635 (2001).

6 Mähönen, A. P. *et al.* A novel two-component hybrid molecule regulates vascular morphogenesis of the Arabidopsis root. *Genes Dev* **14**, 2938-2943 (2000).

7 Mähönen, A. P. *et al.* Cytokinin signaling and its inhibitor AHP6 regulate cell fate during vascular development. *Science* **311**, 94-98, doi:10.1126/science.1118875 (2006).

8 Bishopp, A. *et al.* A mutually inhibitory interaction between auxin and cytokinin specifies vascular pattern in roots. *Curr Biol* **21**, 917-926, doi:10.1016/j.cub.2011.04.017 (2011).

9 De Rybel, B. *et al.* Plant development. Integration of growth and patterning during vascular tissue formation in Arabidopsis. *Science* **345**, 1255215, doi:10.1126/science.1255215 (2014).

10 Vatén, A. *et al.* Callose biosynthesis regulates symplastic trafficking during root development. *Dev Cell* **21**, 1144-1155, doi:10.1016/j.devcel.2011.10.006 (2011).

11 Brady, S. M. *et al.* A high-resolution root spatiotemporal map reveals dominant expression patterns. *Science* **318**, 801-806, doi:10.1126/science.1146265 (2007).

12 Yanagisawa, S. The Dof family of plant transcription factors. *Trends Plant Sci* **7**, 555-560 (2002).

13 Rueda-Romero, P., Barrero-Sicilia, C., Gómez-Cadenas, A., Carbonero, P. & Oñate-Sánchez, L. Arabidopsis thaliana DOF6 negatively affects germination in non-after-ripened seeds and interacts with TCP14. *J Exp Bot* **63**, 1937-1949, doi:10.1093/jxb/err388 (2012).

14 Skirycz, A. *et al.* DOF transcription factor AtDof1.1 (OBP2) is part of a regulatory network controlling glucosinolate biosynthesis in Arabidopsis. *Plant J* **47**, 10-24, doi:10.1111/j.1365-313X.2006.02767.x (2006).

15 Guo, Y., Qin, G., Gu, H. & Qu, L. J. Dof5.6/HCA2, a Dof transcription factor gene, regulates interfascicular cambium formation and vascular tissue development in Arabidopsis. *Plant Cell* **21**, 3518-3534, doi:10.1105/tpc.108.064139 (2009).

16 Schlereth, A. *et al.* MONOPTEROS controls embryonic root initiation by regulating a mobile transcription factor. *Nature* **464**, 913-916, doi:10.1038/nature08836 (2010).

17 Wallner, E. S. *et al.* Strigolactone- and Karrikin-Independent SMXL Proteins Are Central Regulators of Phloem Formation. *Curr Biol* **27**, 1241-1247, doi:10.1016/j.cub.2017.03.014 (2017).

18 Mähönen, A. P. *et al.* Cytokinins regulate a bidirectional phosphorelay network in Arabidopsis.

Curr Biol **16**, 1116-1122, doi:10.1016/j.cub.2006.04.030 (2006).

19 Kiba, T., Aoki, K., Sakakibara, H. & Mizuno, T. Arabidopsis response regulator, ARR22, ectopic expression of which results in phenotypes similar to the wol cytokinin-receptor mutant. *Plant Cell Physiol* **45**, 1063-1077, doi:10.1093/pcp/pch128 (2004).

20 Prigge, M. J. *et al.* Class III homeodomain-leucine zipper gene family members have overlapping, antagonistic, and distinct roles in Arabidopsis development. *Plant Cell* **17**, 61-76, doi:10.1105/tpc.104.026161 (2005).

21 Carlsbecker, A. *et al.* Cell signalling by microRNA165/6 directs gene dose-dependent root cell fate. *Nature* **465**, 316-321, doi:10.1038/nature08977 (2010).

22 Miyashima, S., Koi, S., Hashimoto, T. & Nakajima, K. Non-cell-autonomous microRNA165 acts in a dose-dependent manner to regulate multiple differentiation status in the Arabidopsis root. *Development* **138**, 2303-2313, doi:10.1242/dev.060491 (2011).

23 Baima, S. *et al.* The expression of the Athb-8 homeobox gene is restricted to provascular cells in Arabidopsis thaliana. *Development* **121**, 4171-4182 (1995).

24 Donner, T. J., Sherr, I. & Scarpella, E. Regulation of preprocambial cell state acquisition by auxin signaling in Arabidopsis leaves. *Development* **136**, 3235-3246, doi:10.1242/dev.037028 (2009).

25 O'Malley, R. C. *et al.* Cistrome and Epicistrome Features Shape the Regulatory DNA Landscape. *Cell* **166**, 1598, doi:10.1016/j.cell.2016.08.063 (2016).

26 Gaudinier, A. *et al.* Enhanced Y1H assays for Arabidopsis. *Nat Methods* **8**, 1053-1055, doi:10.1038/nmeth.1750 (2011).

27 Muraro, D. *et al.* Integration of hormonal signaling networks and mobile microRNAs is required for vascular patterning in Arabidopsis roots. *Proc Natl Acad Sci U S A* **111**, 857-862, doi:10.1073/pnas.1221766111 (2014).

28 Mellor, N. *et al.* Theoretical approaches to understanding root vascular patterning: a consensus between recent models. *J Exp Bot* **68**, 5-16, doi:10.1093/jxb/erw410 (2017).

29 De Rybel, B., Mähönen, A. P., Helariutta, Y. & Weijers, D. Plant vascular development: from early specification to differentiation. *Nat Rev Mol Cell Biol* **17**, 30-40, doi:10.1038/nrm.2015.6 (2016).

30 Fauser, F., Schiml, S. & Puchta, H. Both CRISPR/Cas-based nucleases and nickases can be used efficiently for genome engineering in Arabidopsis thaliana. *Plant J* **79**, 348-359, doi:10.1111/tpj.12554 (2014).

31 Lei, Y. *et al.* CRISPR-P: a web tool for synthetic single-guide RNA design of CRISPR-system in plants. *Mol Plant* **7**, 1494-1496, doi:10.1093/mp/ssu044 (2014).

32 Wysocka-Diller, J. W., Helariutta, Y., Fukaki, H., Malamy, J. E. & Benfey, P. N. Molecular analysis of SCARECROW function reveals a radial patterning mechanism common to root and shoot. *Development* **127**, 595-603 (2000).

33 Kurihara, D., Mizuta, Y., Sato, Y. & Higashiyama, T. ClearSee: a rapid optical clearing reagent for whole-plant fluorescence imaging. *Development* **142**, 4168-4179, doi:10.1242/dev.127613 (2015).

34 Siligato, R. *et al.* MultiSite Gateway-Compatible Cell Type-Specific Gene-Inducible System for

Plants. *Plant Physiol* **170**, 627-641, doi:10.1104/pp.15.01246 (2016).

35 Hashimoto, K., Miyashima, S., Sato-Nara, K., Yamada, T. & Nakajima, K. Functionally Diversified Members of the MIR165/6 Gene Family Regulate Ovule Morphogenesis in Arabidopsis thaliana. *Plant Cell Physiol* **59**, 1017-1026, doi:10.1093/pcp/pcy042 (2018).

36 Hejátko, J. *et al.* In situ hybridization technique for mRNA detection in whole mount Arabidopsis samples. *Nat Protoc* **1**, 1939-1946, doi:10.1038/nprot.2006.333 (2006).

37 Wickham, H. & Sievert, C. *ggplot2 : elegant graphics for data analysis*. Second edition. edn, (Springer, 2016).

38 De Rybel, B. *et al.* A bHLH complex controls embryonic vascular tissue establishment and indeterminate growth in Arabidopsis. *Dev Cell* **24**, 426-437, doi:10.1016/j.devcel.2012.12.013 (2013).

39 Oparka, K. J., Duckett, C. M., Prior, D. A. M. & Fisher, D. B. Real - time imaging of phloem unloading in the root tip of Arabidopsis. *The Plant Journal* **6**, 759-766, doi:doi:10.1046/j.1365-313X.1994.6050759.x (1994).

40 Digman, M. A. *et al.* Measuring fast dynamics in solutions and cells with a laser scanning microscope. *Biophys J* **89**, 1317-1327, doi:10.1529/biophysj.105.062836 (2005).

41 Clark, N. M. *et al.* Tracking transcription factor mobility and interaction in Arabidopsis roots with fluorescence correlation spectroscopy. *Elife* **5**, doi:10.7554/eLife.14770 (2016).

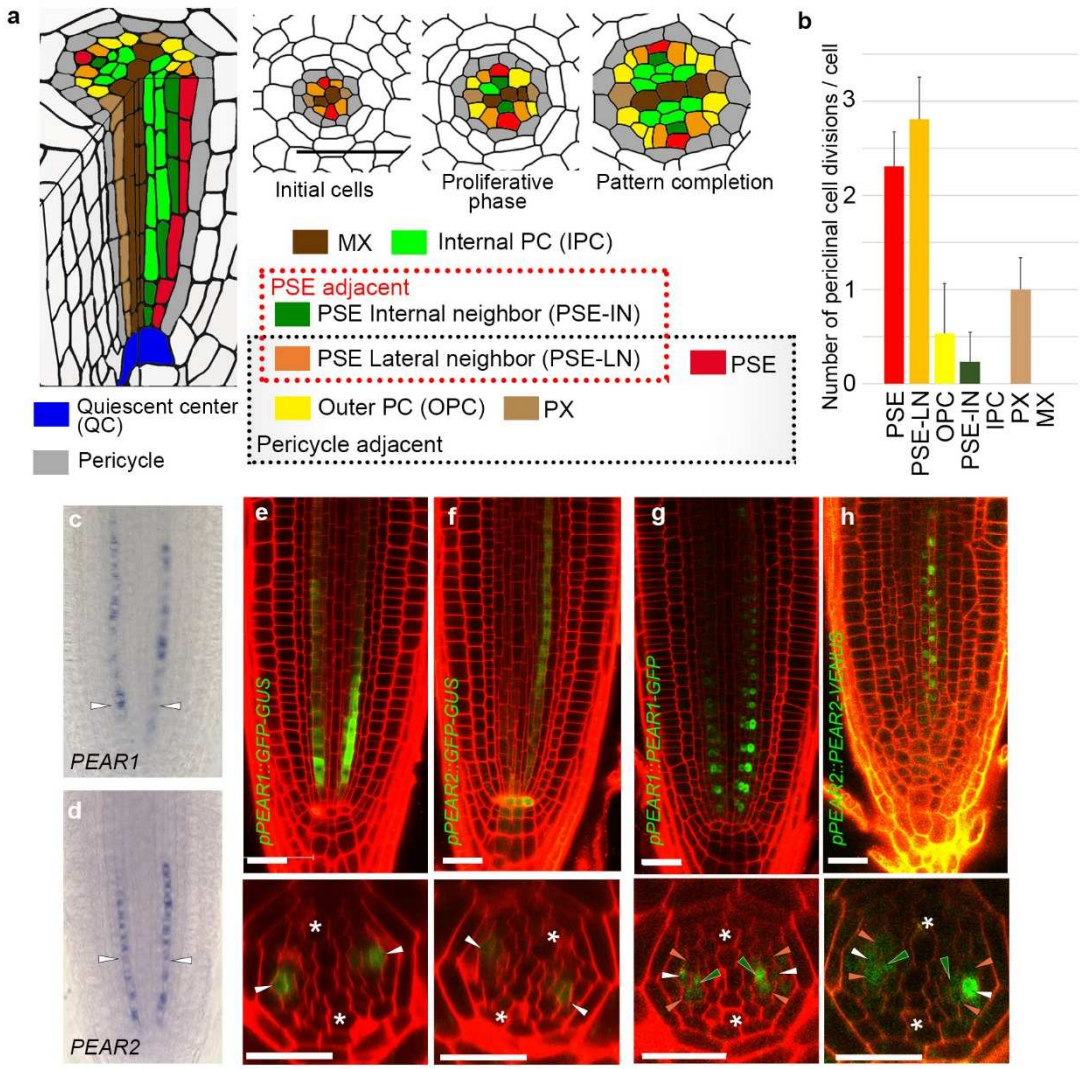

Figure 1| Periclinal cell divisions are centered around PSE, a domain highlighted by a pair of mobile DOF transcription factors, PEAR1 and PEAR2.

a, Schematic representation of procambial cells based on the position relative to PSE (red) and outer pericycle (gray). PSE neighboring cells are classified as PSE lateral neighbor (PSE-LN, orange), a cell adjacent to both PSE and pericycle, or PSE internal neighbor (PSE-IN, dark-green), a cell adjacent to PSE but not pericycle. Intervening procambial cells are classified as outer PC (OPC, yellow), a procambial cell adjacent to pericycle, or internal PC (IPC), a procambial cell non-adjacent to pericycle. PX and MX represent protoxylem and metaxylem, respectively. **b**, Number of periclinal cell divisions in each cell during procambial development. PSE and PSE-LN exhibited higher proliferative activity. **c-d**, Whole mount *in situ* hybridization with a PEAR1 (c) and a PEAR2 probe (d) in wild-type root, showing PSE-specific mRNA localization (arrowheads)**. e-f**, Expression of *pPEAR1::GFP-GUS* (c) and *pPEAR2::GFP-GUS* (d). Both transcriptional fusions exhibit a highly PSE-specific expression pattern in the vascular tissue, though a residual level of GFP signal was observed in PSE-IN, most likely due to the retention of fluorescent protein after the division of PSE. **g-h**, Expression of the translational fusions of PEAR1 to GFP (e) and PEAR2 to VENUS (f). Fluorescent signal is observed not only in PSE but also in its neighboring cells, including PSE-LN and PSE-IN. White, dark-green, orange arrowheads and asterisks indicates PSE, PSE-IN,PSE-LN and protoxylem, respectively. Scale bars, 25 μm.

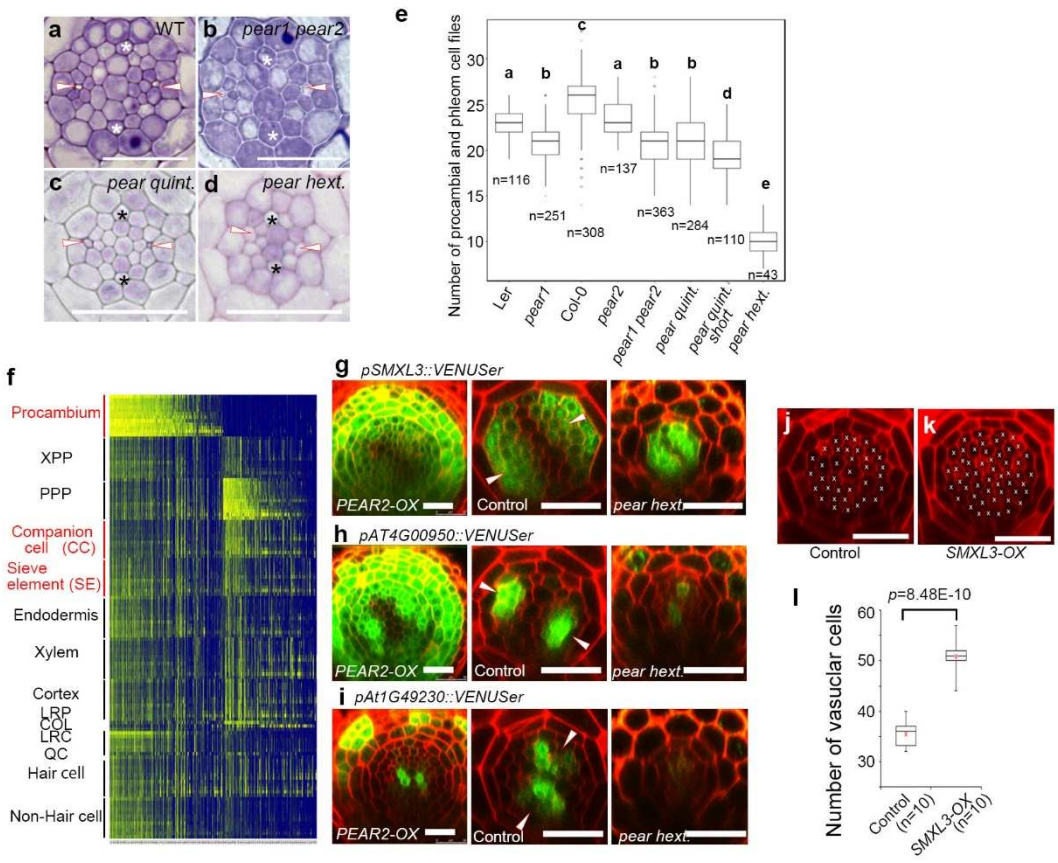

Figure 2| PEAR genes activate periclinal cell division by controlling downstream genes in non-cell autonomous manner.

a-d, Cross-section of wild type (a), *pear1 pear2* (b), *pear* quintuple (*pear1 pear2 dof6 obp2 hca2*) (c) and *pear* hextuple (*pear1 pear2 dof6 obp2 hca2 tmo6*) (d), respectively. **e**, Number of procambial and phloem cell files in wild type and *pear* combinatorial mutants. Values were calculated from root cross sections at the differentiation zone. Sample size is given below each bar. Tukey statistical test $p<0.05$. **f,** Heatmap showing the predicted spatiotemporal expression patterns of all genes induced by PEAR1 or PEAR2. **g-i,** Expression of selected PEAR1/2 downstream genes in wild type, PEAR2 overexpression plant and *pear* hextuple mutant. *SMXL3* is expressed in phloem and procambial tissue, whose expression induced by PEAR2 overexpression, but not altered in *pear* hextuple (g). *AT4G00950* gene is expressed in PSE and its neighboring cells, whose expression is induced by PEAR2 overexpression and reduced in *pear* hextuple (h). *AT1G49230* gene is expressed in PSE-neighboring cells and procambial cells, but not PSE itself. In a similar manner to AT4G00950, its expression is induced by PEAR2 overexpression and reduced in the *pear* hextuple mutant (i). **j-l,** Overexpression of SMXL3 increases vascular cell number. White arrowheads and asterisks indicate PSE and protoxylem cell, respectively. Scale bars, 25 μm

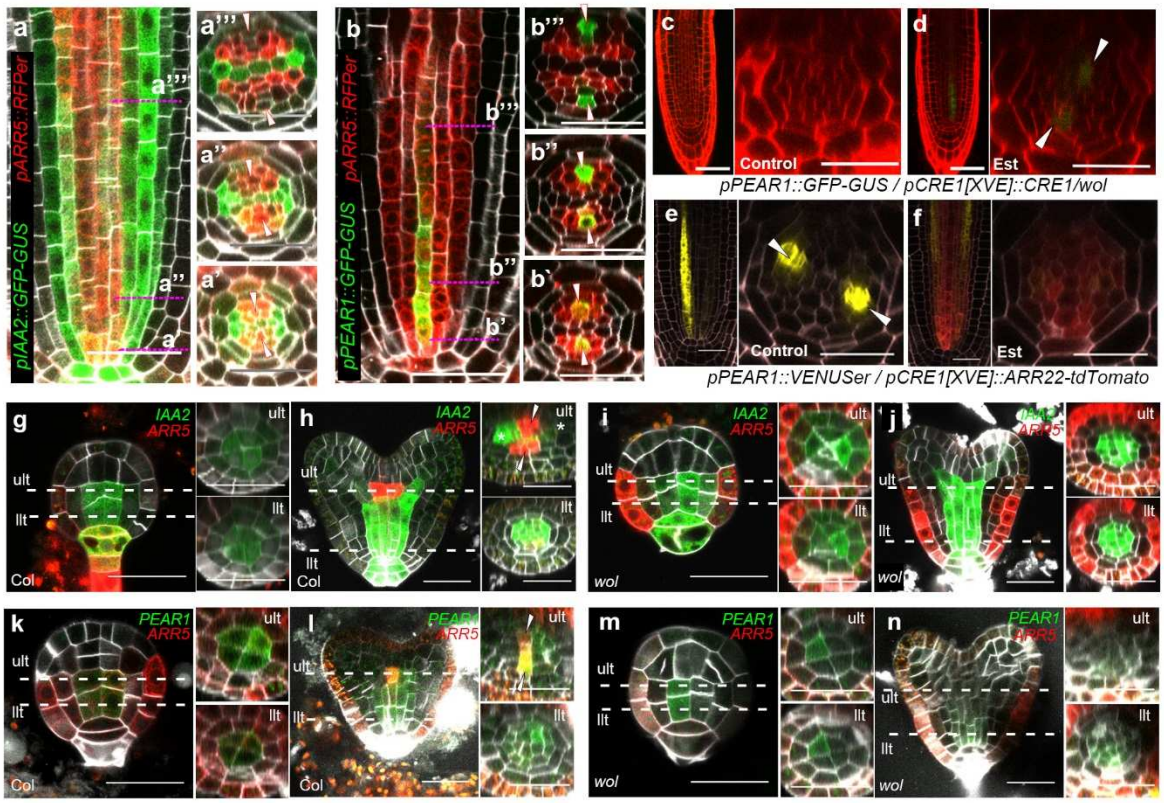

Figure 3|Cytokinin signalling triggers PEAR1 expression in the embryonic root and maintain its post-embryonic expression.

a, Expression of auxin (*pIAA2::GFP-GUS)* and cytokinin (*pARR5::RFPer*) response genes. Auxin response is restricted to the xylem cells at initial stage (a') and maintained during development (a''-a'''). High cytokinin response is activated initially and maintained in PSE and its neighboring cell (a' and aa'), and later becomes concentrated into the intervening procambial cells flanking to xylem cells (a'''). **b,** Expression of *ARR5* and *PEAR1* expression overlaps at initial stage (b') and early proliferative phase (b''). **c-d**, Transcription of PEAR1 in *wol* root which is conditionally rescued by CRE1 induction. *PEAR1* transcription severely attenuate in the condition attenuated cytokinin response (c), and is restored after three days induction of *CRE1* (d, arrowheads). **e-f,** PEAR1 transcription is down-regulated after 48 hours of *ARR22* induction (e). **g-i,** Expression of *pIAA2::GFP-GUS* and *pARR5::RFPer* during embryogenesis in wild type (f-g) and in *wol* (h-i). At the globular stage, auxin response is activated among vascular cells both in wild type (g) and in *wol* (i). At the early heart stage, cytokinin response is activated in cells positioned below the shoot apical meristem (h, ult, arrowheads), but this does not occur in *wol* (j). **k-n**, Expression of *pARR5::RFPer* and *pPEAR1::GFP-GUS* during embryogenesis in wild type (k-l) and in *wol* (m-n). *PEAR1* is transcribed among the provascular cells at the globular-stage embryo in both backgrounds (k and m). At the heart-stage, *PEAR1* transcription is activated in ult cells underneath the shoot apical meristem, which is correlated with the activation of cytokinin response in this domain (l, arrowheads), but does not occur in *wol* (n). ult, upper lower tier; llt, lower lower tier; Scale bars, 25 μm.

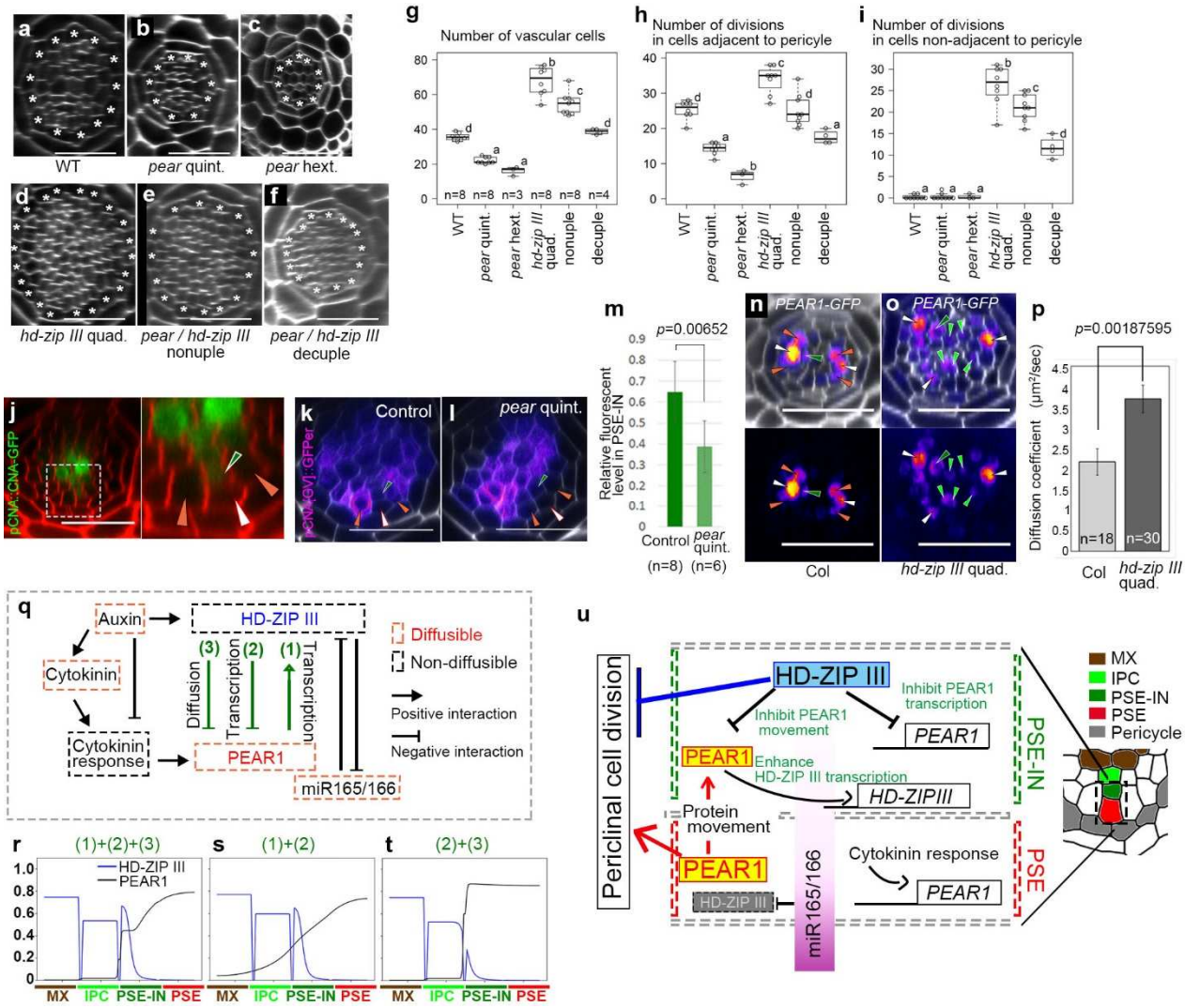

Figure 4| Antagonistic function of PEAR1 and HD-ZIP III sharpens the boundary between dividing and non-dividing cells.

a-f, An optical cross-section image of vascular tissue in wild type (a), *pear* quintuple (b), *pear* hextuple (c), *hd-zip III* quadruple (d), *pear hd-zip III* nonuple (e) and *pear hd-zip III* decuple mutant (f). Asterisks indicate pericycle cells. **g-i,** Quantification of vascular cell number (g), and the number of periclinal cell divisions in cells adjacent (h) or non-adjacent to pericycle (i). In the analysis of *pear* quintuple and *pear hd-zip III* nonuple, a population of slowly elongating roots is selected as described in Fig. 2e. Tukey statistical test $p<0.05$. Sample size is given below. **j**, CNA protein is eliminated in both PSE and PSE-LN, but retained in PSE-IN. **k-l**, Expression of CNA transcriptional reporter in the control (k, the heterozygous *pear* quintuple) and *pear* quintuple background (l). Fluorescent level in PSE-IN (dark-green arrowheads) is significantly reduced in *pear* quintuple (m). **n-o,** PEAR1-GFP localization in wild type (n) and *hd-zip III* quadruple mutant (o). PEAR1-GFP is broadly localized even in IPC in *hd-zip III* quadruple (o, light-green arrowheads). **p**, Average diffusion coefficient of PEAR1-GFP in wild type and *hd-zip III* quadruple root obtained by performing Raster Image Correlation Spectroscopy (RICS). Error bars are s.e.m. **q,** Regulatory network embedded as differential equations within each spatial compartment in the model. **r,** Including all three interactions labeled in panel q in the model, results in the formation of sharp concentration gradients of PEAR1 (black line) and HD-ZIP III (blue line) with the boundary forming in the PSE-IN. **s,** In simulations where HD-ZIP III does not regulate PEAR1 diffusion (Interaction (3) in Fig. 4q), PEAR1 protein is predicted to spread

into the procambium and metaxylem as shown in Fig. 4o. **t,** In simulations where PEAR1 does not activate HD-ZIP III transcription (Interaction (1) in Fig. 4q), the concentration of HD-ZIP III is reduced in the PSE-IN cell as shown in Fig. 4l. **u,** A regulatory mechanism forming the boundary between a dividing and a non-dividing cell during procambial development. White, orange, dark-green and light-green arrowheads indicate PSE, PSE-LN, PSE-IN and IPC. Scale bars, 25 μm.

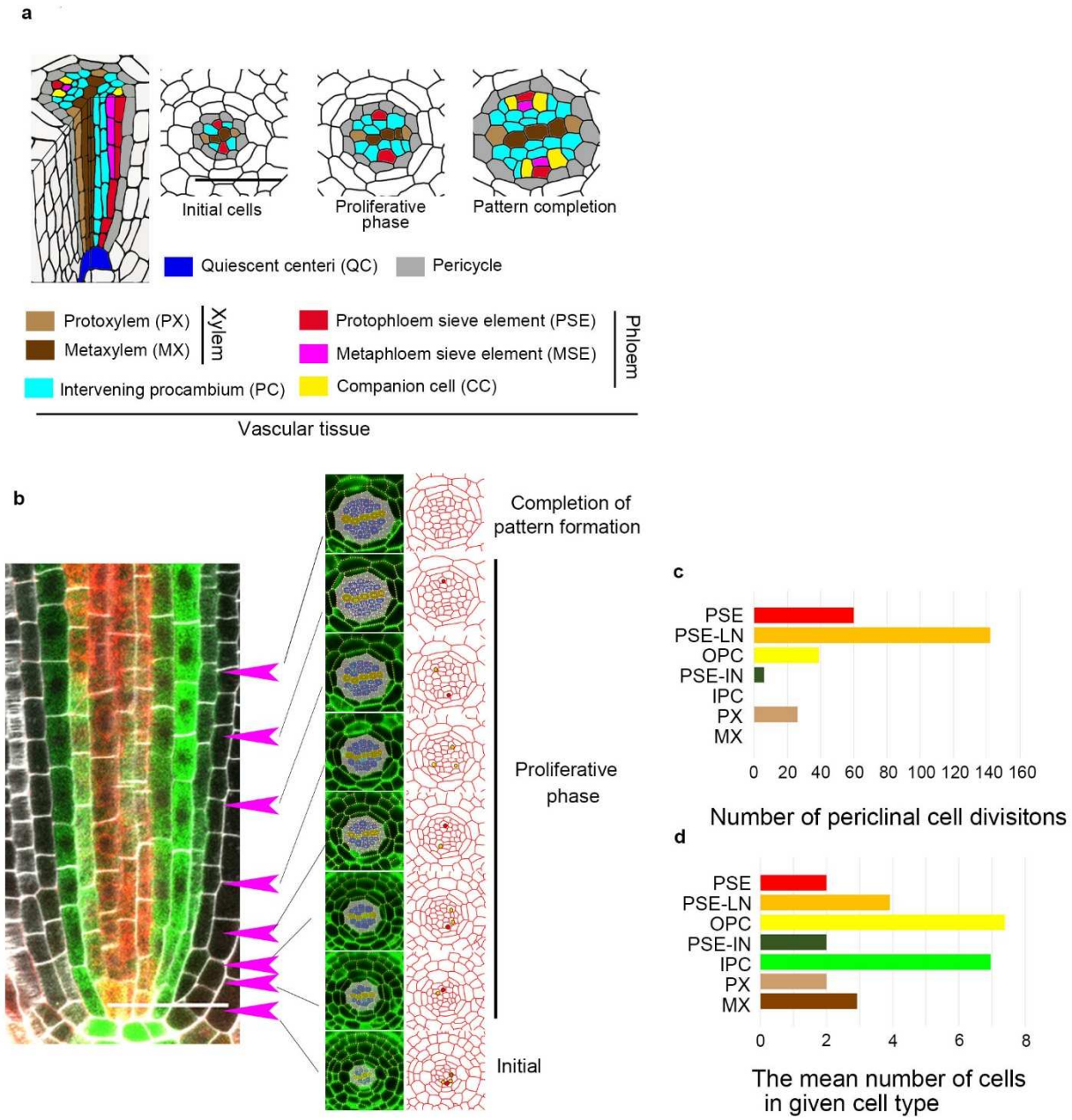

Extended Data Fig. 1| Quantification of periclinal cell division during procambial development. **a**, Schematic representation of root vascular tissue of Arabidopsis. Procambial cells originate from their initial cells, and periclinal cell division increases the cell files during the proliferative phase, and eventually results in a bisymmetric vascular pattern, composed of a pair of phloem poles which are separated from central xylem axis by intervening procambium. **b**, An example of mapping the position of periclinal cell division from the initial cells. From each position within the root vascular tissue (arrows), an optical cross-section image is constructed, and cells were segmented using CellSet. **c**, The number of periclinal cell division in each cell position (273 division events from 13 independent roots). **d**, The mean cell number in each category during procambial development. The number of events per cell in each group was calculated by diving the number of events by the mean cell number of each group during development (See Supplementary Information).

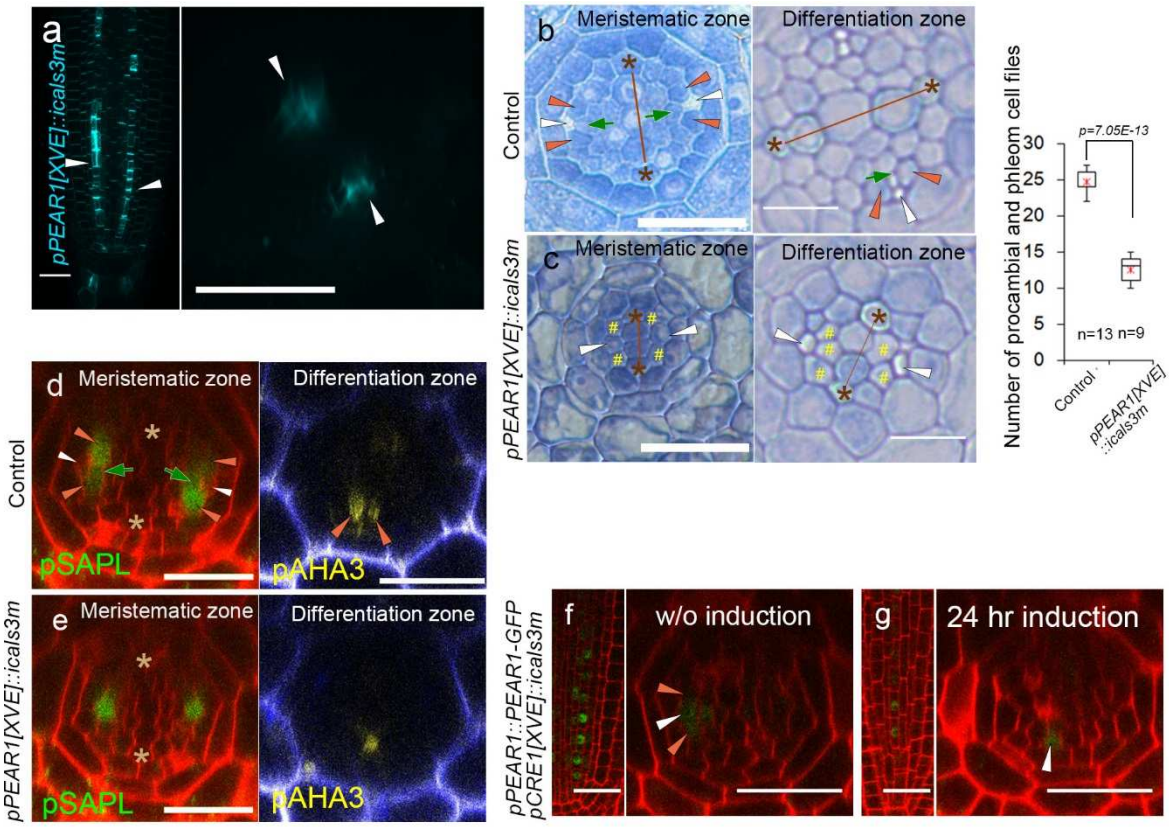

Extended Data Fig. 2| Inhibition of symplastic connection in early PSE results in the reduction of vascular cell number and in PSE-specific PEAR1-GFP localization.

a, Aniline blue stained primary root of *pPEAR1[XVE]::icals3m* after 24 hours of induction. Callose deposition occurs superficially in PSE cells (arrowheads). **b-c,** The vascular tissue of *pPEAR1[XVE]::icals3m* root, in non-induced (b) and after three days induction (c). In non-induced condition, PSE cells (white arrowheads) and their neighboring cells, composed of MSE (dark-green arrows) and two lateral companion cells (orange arrowheads), are spatially separated from the xylem axis by intervening procambium. By contrast, after three days induction of callose deposition in PSE cells, only a single SE cell file is formed in each phloem pole (c, white arrowheads), and its neighboring cells often touch the xylem axis (c, yellow hashtags). Number of procambial and phloem cell files is significantly reduced after three days induction. **d-e**, Expression of *Sister of APL* (*SAPL*, AT3G12730) and *ATPase 3 (AHA3*, AT5G57350) in *pPEAR1[XVE]::icals3m* before (d) or after 24 hours of induction (e). *SAPL* is expressed in CC and MSE in meristematic zone, and *AHA3* is expressed in differentiated CC (d). After 24 hours of induction, expression of these genes is restricted to a single cell file, indicating that symplastic cell communication between PSE and PSE-LN is required for the specification of PSE-neighboring cell identity. **f-g**, PEAR1-GFP localization in *pCRE1[XVE]::icals3m* before (f) or after 24 hours of induction (g). PEAR1-GFP becomes specific to PSE cell after the induction of callose deposition in whole vascular tissue (g), suggesting that PEAR1-GFP move in a short rage via plasmodesmata. White, orange and dark-green arrowheads indicate PSE, PSE-LN and PSE-IN, respectively. Asterisks indicate protoxylem (PX) cells.

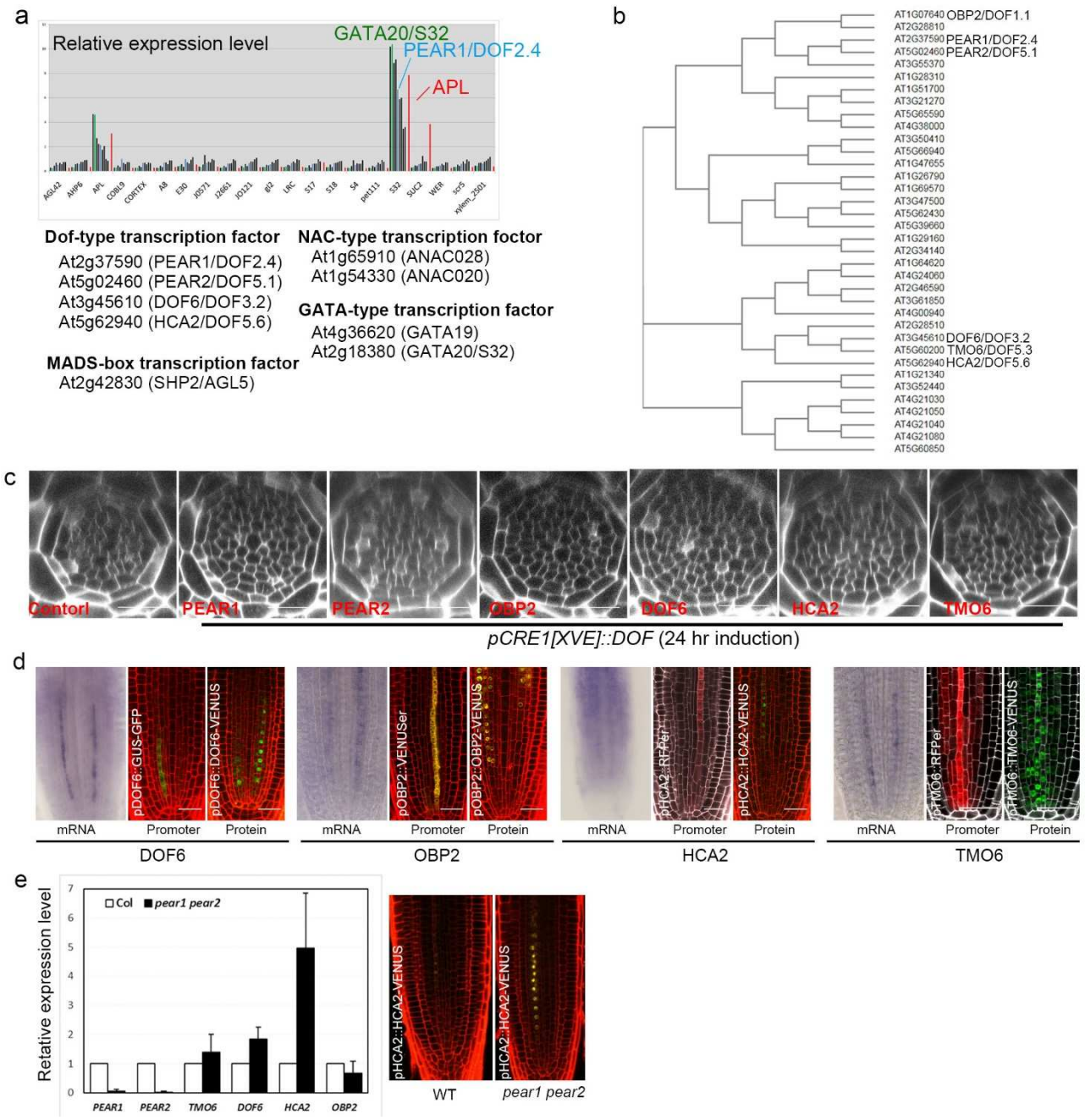

Extended Data Fig. 3| Identification of PEAR genes

a, *In silico* analysis of the early phloem abundant transcription factors. Nine transcription factors are shown to be expressed abundantly in the early phloem cell (S32 fraction), containing four types of transcription factors, including DOF-type, MADS-box, NAC-type and GATA-type transcription factors. **b**, A phylogenetic tree of 36 Arabidopsis DOF transcription factors is drawn using Clustal Omega (https://www.ebi.ac.uk/Tools/msa/clustalo/). **c,** Overexpression of *PEAR* genes, including *PEAR1*, *PEAR2*, *OBP2*, *DOF6*, *HCA2* and *TMO6*, under the *CRE1* inducible promoter enhances the periclinal cell division in the vascular tissue. **d**, Expression of four *PEAR* genes, including *DOF6, OBP2, HCA2 and TMO6. DOF6* and *OBP2*, show similar expression patterns to PEAR1, in which both mRNA and transcriptional fusion reporter exhibit PSE-specific pattern with a broad protein localization. HCA2 translational fusion in wild-type background exhibits weak and specific pattern in PSE, but its expression level is enhanced in *the pear* quintuple mutant background (see Supplemental Notes). Though TMO6 mRNA is highly specific to PSE cells, its transcriptional fusion reporter shows the broad but PSE abundant expression pattern with a broad TMO6 protein localization. **e**, A

quantitative analysis of PEAR transcripts in *pear1 pear2* double mutant background. Note that the level of transcripts of three *PEAR* genes, including *TMO6*, *DOF6* and *HCA2*, is elevated in *pear1 pear2* background, suggesting that a compensation mechanism would mask the effect of *pear1 pear2* loss of function (also see Supplemental Information).

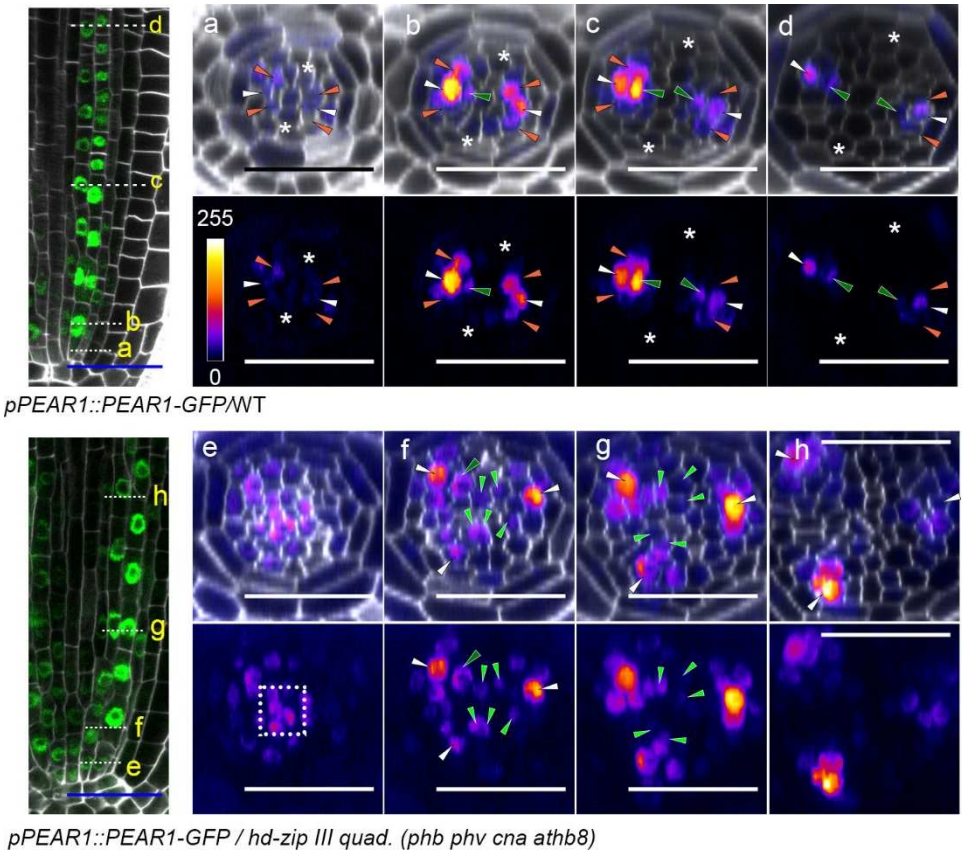

Extended Data Fig. 4| PEAR1-GFP localization during procambial development

a-d, PEAR1-GFP localization in wild-type background. The position of each optical section is indicated in the left panel showing the longitudinal section. At the position of the vascular initial cells, weak PEAR1-GFP signal is observed in PSE and neighboring procambial cells but not in the xylem cells (a). During an early stage of the proliferative phase, the highest PEAR1-GFP signal is detected in the PSE, and substantial level of PEAR1-GFP signal is observed in PSE neighboring cells, PSE-LN and PSE-IN (b, c) and its expression is maintained by the end of proliferation stage (d), indicating that the expression pattern of PEAR1-GFP is correlated with the domain having high proliferative activity, except for PSE-IN where almost no periclinal cell division is detected (see Fig. 1). **e-f,** PEAR1-GFP localization in *hd-zip III* quadruple (*phb phv cna athb8*) mutant background. The position of each optical section is indicated in left panel showing the longitudinal section. Broad localization of PEAR1-GFP is detected at the level of vascular initials. Central domain is highlighted with dotted square (e). At the early stage of proliferative stage, fluorescent signal is detected in IPC cells (light-green arrowheads), as well as PSE and its neighboring cells (f, g), and gradually becomes specific to PSE and its neighbors (h). White, orange and dark-green and light-green arrowheads indicate PSE, PSE-LN, PSE-IN and IPC respectively. Scale bars represent 25 μm.

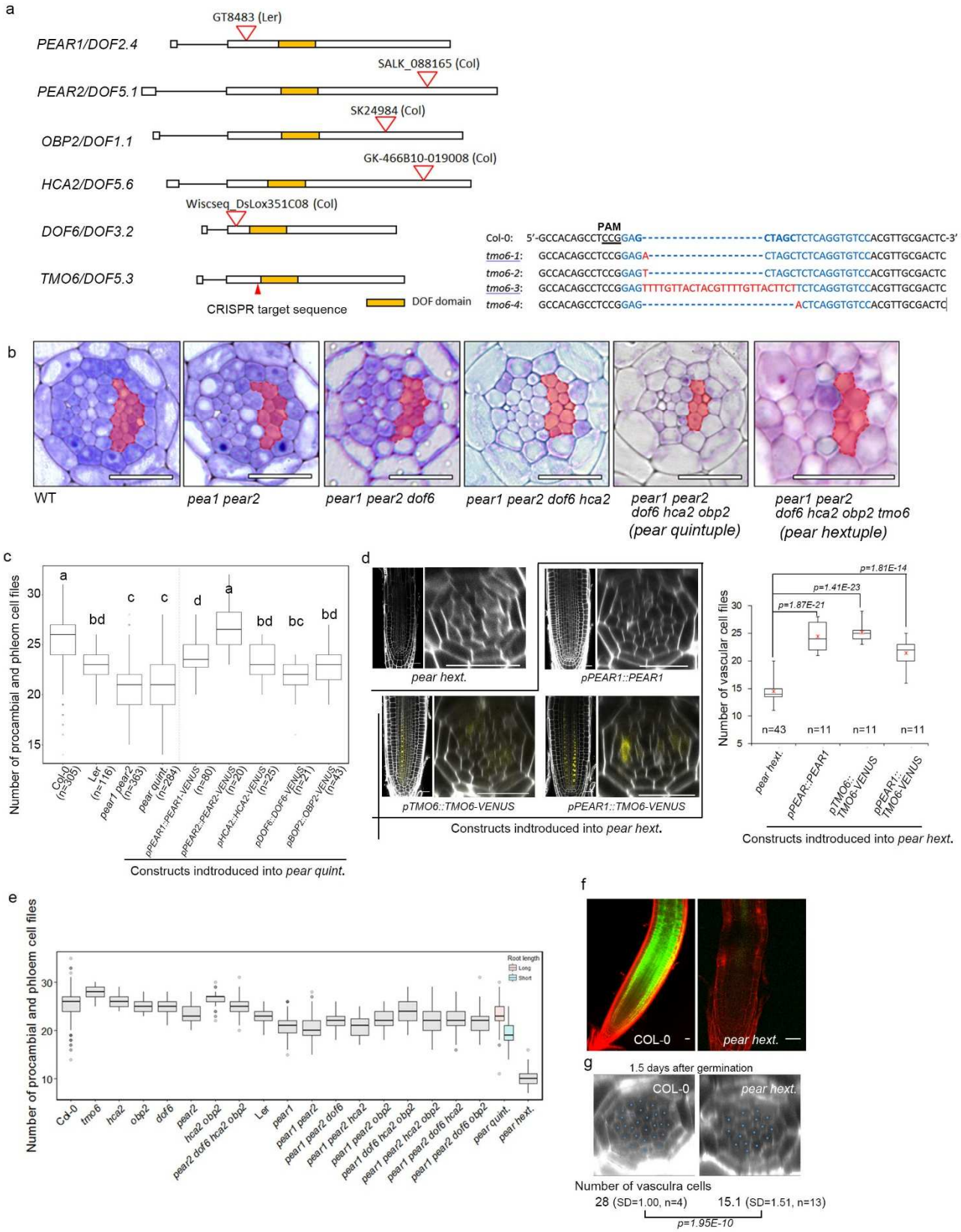

Extended Data Fig. 5| Loss of function of PEAR genes.

a, Organization of PEAR genes and CRISPR/Cas9-induced mutation in TMO6 locus. Deletions are denoted by dashes; insertions and a replacement are indicated by red letters. **b,** Cross-section image of *pear* mutant combination. Phloem and procambial cells are indicated in red. **c,** *pear* quintuple mutant phenotype is fully (PEAR1 and PEAR2) or partially (HCA2 and OBP2) rescued by introduction of fluorescent-tagged PEAR proteins expressed under their native promoters. Tuckey statistical test $p<0.05$. **d,** Introduction of PEAR1 (*pPEAR1::PEAR1*), TMO6 (*pTMO6::TMO6-VENUS*) or PSE-specifically transcribed TMO6 (*pPEAR1::TMO6-VENUS*) construct significantly increases vascular

cell number of *pear* hextuple. **e,** Quantification of vascular cell number in each *pear* mutant combination. **f,** Phloem unloading assay in wild type and *pear* hextuple. Fluorescent CFDA dye is loaded on the cotyledon and imaged 2 hours after application (see Methods). No phloem transport is observed in *pear* hextuple. **g,** Phenotype of *pear* hextuple mutant at the early developmental stage (1.5 days after germination). The cell number in vascular tissue of *pear* hextuple is significantly reduced before the onset of phloem PSE differentiation and activation of the phloem transport (see SI). Scale bars represent 25 μm.

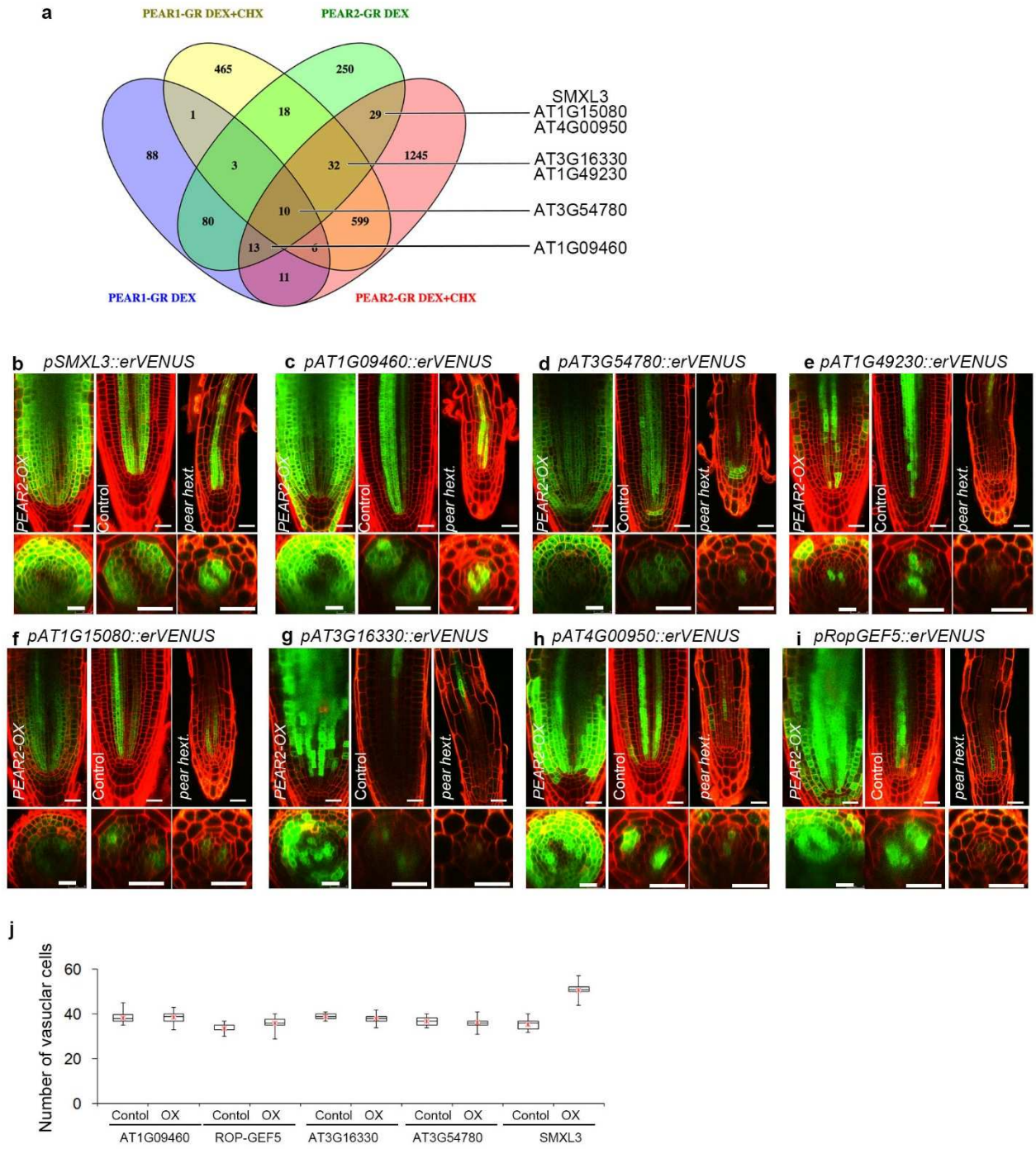

Extended Data Fig. 6| Identification of genes acting downstream of PEAR

a, Venn diagrams showing the genes upregulated by overexpression of *PEAR1* (left panel) or *PEAR2* (right panel), and the overlap between them (lower panel). The analysis revealed 212 and 435 genes directly up-regulated, in the respective experiments. **b-i**, Expression pattern of eight selected genes responding to *PEAR2* overexpression. In control conditions, all genes exhibit a broad expression pattern, in which five of them are transcribed both in phloem and procambial cells (b-d and i), and the rest of them are in PSE and its surrounding cells where PEAR proteins are accumulated abundantly (e-h). Whereas expression of SMXL3, AT1G09460 and AT1G15080 are maintained even in *pear* hextuple (b, c, f), the expression level of five genes are attenuated (d, e, g-i). **j**, Number of vascular cells after 3-days induction of overexpression of each PEAR downstream gene. Only *SMXL3* overexpression can increase the vascular cell number (n>12, for each sample). Scale bars represent 25 μm.

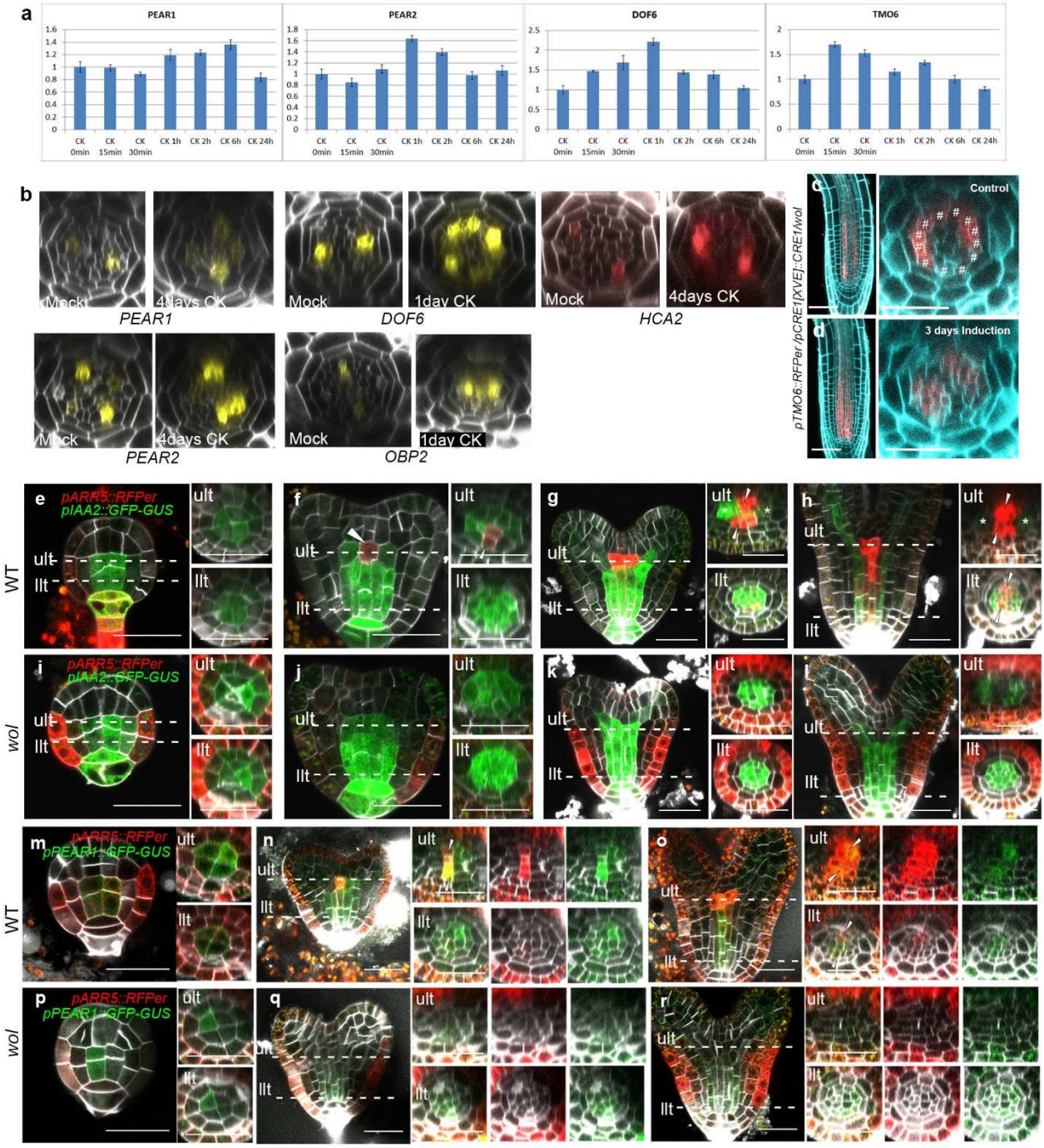

Extended Data Fig. 7| Cytokinin controls PEAR expression.

a, Exogenous cytokinin application rapidly promotes the transcript level of *PEAR* genes, including *PEAR1*, *PEAR2*, *DOF6*, and *TMO6*. **b**, Sustained cytokinin application leads to the ectopic transcription of *PEAR* genes. The optical cross section images are obtained after 4 days (for *PEAR1*, *PEAR2* and *HCA2*) or 1-day (*DOF6* and *OBP2*) treatment of 1μM of BA. **c-d**, Conditional induction of *CRE1* expression restores *TMO6* transcription in *wol* root. In the absence of cytokinin response, TMO6 transcription is restricted to pericycle (c, hashtags), and restored in the vascular tissue after CRE1 induction (d). **e-l**, Expression pattern of auxin (*pIAA2::GFP-GUS*) and cytokinin (*pARR5::RFPer*) response reporters during embryogenesis in wild type (c-h) and *wol* (i-l). At globular stage, auxin response is activated among provascular cells both in wild type (f) and in *wol* (j). At early heart stage, cytokinin response is activated in cells positioned below shoot apical meristem (f, ult, arrowheads), and the stripe of cytokinin response domain is formed by mid heart stage (g, ult, arrowheads), simultaneously auxin response becomes concentrated in the cells proximal to the

cotyledon (g, ult, asterisks), resulting in the bisymmetric hormonal response pattern. During the torpedo stage, cytokinin response domain reaches to llt (h, llt, arrowheads). In *wol* embryos, activation of cytokinin response in vascular tissue does not occur and a radial auxin response pattern is maintained (i-l). **m-r,** Expression of *ARR5* and *PEAR1* during embryogenesis. In the wild-type embryo (o-q), *PEAR1* is broadly transcribed among provascular cells both in ult and llt with radial symmetric pattern at the globular stage (m). In the heart stage, *PEAR1* transcription is enhanced in ult cells underneath the shoot apical meristem, which correlated with the activation of cytokinin response in this domain (n, arrowheads), and expression of both *ARR5* and *PEAR1* extends rootward and reaches to llt, becoming more concentrated within the cell files where phloem is specified post-embryonically (o, arrowheads). In *wol* embryos, *PEAR1* transcription is initiated among provascular cells at the globular embryo stage (p) similar to wild type (m), but neither cytokinin response nor *PEAR1* transcription occurs in ult in the heart stage (q), and *PEAR1* expression is gradually attenuated by the torpedo stage (r). ult and llt represent upper- and lower tier, respectively. Scale bars represent 25 μm.

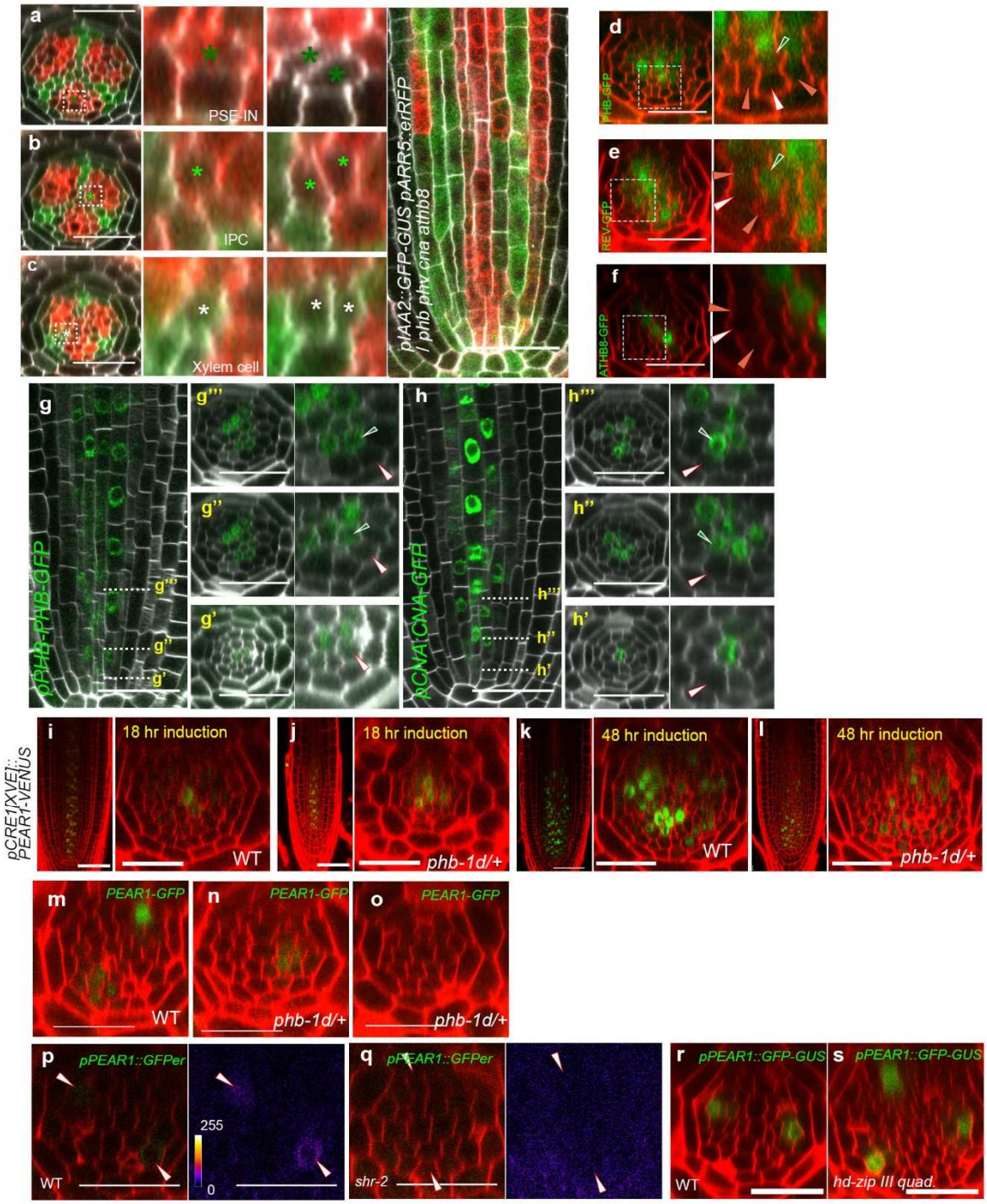

Extended Data Fig. 8| HD-ZIP III restrict periclinal cell divisions during procambial development.

a-c, Periclinal cell divisions in the cells non-adjacent to pericycle, including PSE-IN (a), IPC (b) and xylem cell (c), occurs in *hd-zip III* quadruple (*phb phv cna athb8*). **d-f,** Localization of PHB-GFP (d), REV-GFP (e) and ATHB8-GFP (f). **g-h** Protein localization of PHB-GFP (g) and CNA-GFP (h) during procambial development. In the initial cells (g', h'), both proteins localized in metaxylem cells but not in PSE (white arrowheads). During the proliferation stage, PSE-IN (green arrowheads), which is produced by periclinal cell division in PSE, acquires the expression of both PHB-GFP (g'', g''') and CNA (h'', h'''). **i-l**, Overexpression of PEAR1-VENUS under the *CRE1* inducible promoter in wild type (i, k) or heterozygous *phb-1d* background (*phb-1d*/+, j, l). After 18 hours of induction, PEAR1-YFP signal is detected in both backgrounds (i, j), however, enhanced periclinal divisions are only observed in wild type (i), and not in *phb-1d* (j). Longer induction of PEAR1 overexpression induces

divisions even in *phb-1d* (k, l). **m-o,** *pPEAR1-PEAR1-GFP* expression is reduced in heterozygous *phb-1d/+* background. Most of *phb-1d* heterozygotes exhibited a single PEAR1-GFP expressing pole (n, 72% n=11), and the expression of PEAR1-GFP was almost completely abolished in some roots of *phb-1d* (o, 18% n=11). **p-q,** The expression of *pPEAR1::GFPer* in wild type (p), *shr-2* (q). The fluorescent signal is below the limit of detection in *shr-2* (q). **r-s**, Expression of *pPEAR1::GFP-GUS* in WT (r) and *hd-zip III* quadruple mutant (s) . White, orange and dark-green arrowheads indicate PSE, PSE-LN, PSE-IN respectively. Scale bars represent 25 μm.

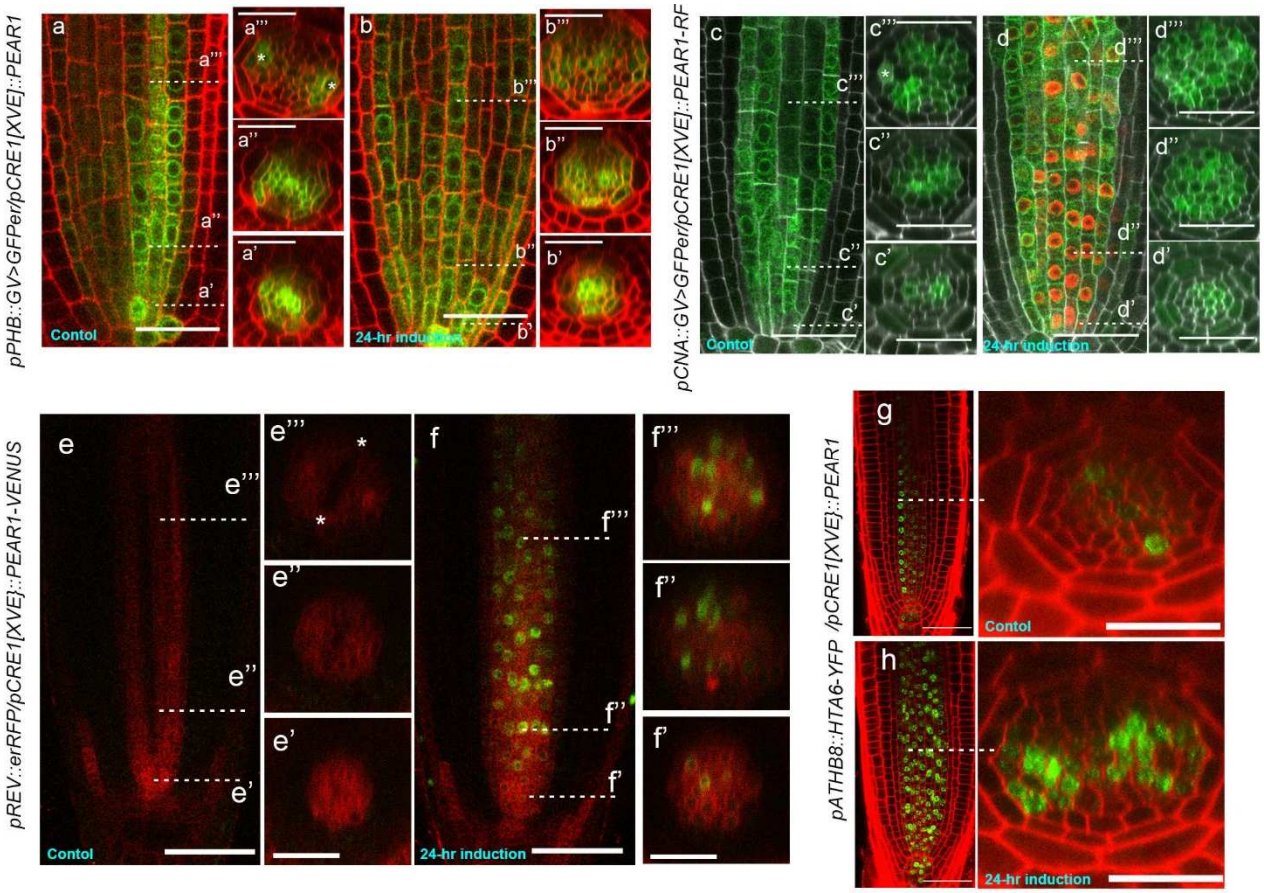

Extended Data Fig. 9| Overexpression of PEAR1 enhances the transcription of HD-ZIP III. The transcription patterns of four HD-ZIP III, including *PHB* (a, b), *CNA* (c, d), *REV* (e, f) and *ATHB8* (g, h) are visualized using their transcriptional fusion constructs. A longitudinal section is shown in the left panel, and the optical cross sections associated with this are shown in the right panels (the position of each section is indicated in the left panel). **a-b**, Transcription pattern of *PHB* (*pPHB::GV>UAS::GFPer*) in *pCRE1[XVE]::PEAR1* plant before (a) and after 24 hours of induction of PEAR1 overexpression (b). PHB transcription is observed in whole vascular tissue at the initial and proliferative phase with peaks in xylem cells (a'), and its expression becomes concentrated into protoxylem cells (a'' and a''', asterisks indicate protoxylem cell). After the induction of PEAR1 overexpression, PHB expression in the central domain of the vascular tissue is maintained at the later stage, resulting in the radially symmetric PHB transcription pattern (b' and b''). **c-d**, Transcription of *CNA* (*pCNA::GV>UAS::GFPer*) in *pCRE1[XVE]::PEAR1-RFP* plant before (c) and after 24 hours of induction (d). CNA transcription is observed mainly in xylem lineage at initial cells (c'), and becomes broader in whole vascular tissue, with peaks in procambial tissue, including PSE neighboring cells (c''), and eventually its expression is gradually reduced in PSE and metaxylem, but is maintained in procambium, PSE neighboring cells, as well as protoxylem cells (c'''). In a similar manner to PHB, CNA transcription in the central domain of the vascular tissue is maintained at the later stage when PEAR1-RFP is overexpressed (d'''). **e-f**, Transcription of REV (*pREV::RFPer*) in *pCRE1[XVE]::PEAR1-VENUS* plant before (e) and after 24 hours of induction (f). REV exhibits distinct transcriptional pattern where its expression is initially uniform in vascular tissue (e'), and highest expression is localized in PSE, while decreasing towards xylem axis (e'' and e'''). When PEAR1-VENUS is overexpressed (f), the transcription pattern of REV is also activated in the central

domain of vascular tissue, resulting in the radial symmetric REV transcription pattern. **g-h**, The expression pattern of *pATHB8::HTA6-YFP* is highly specific to xylem cells (g), and its expression is enhanced after 24 hours of induction of PEAR1 overexpression with a broad expression domain (h).

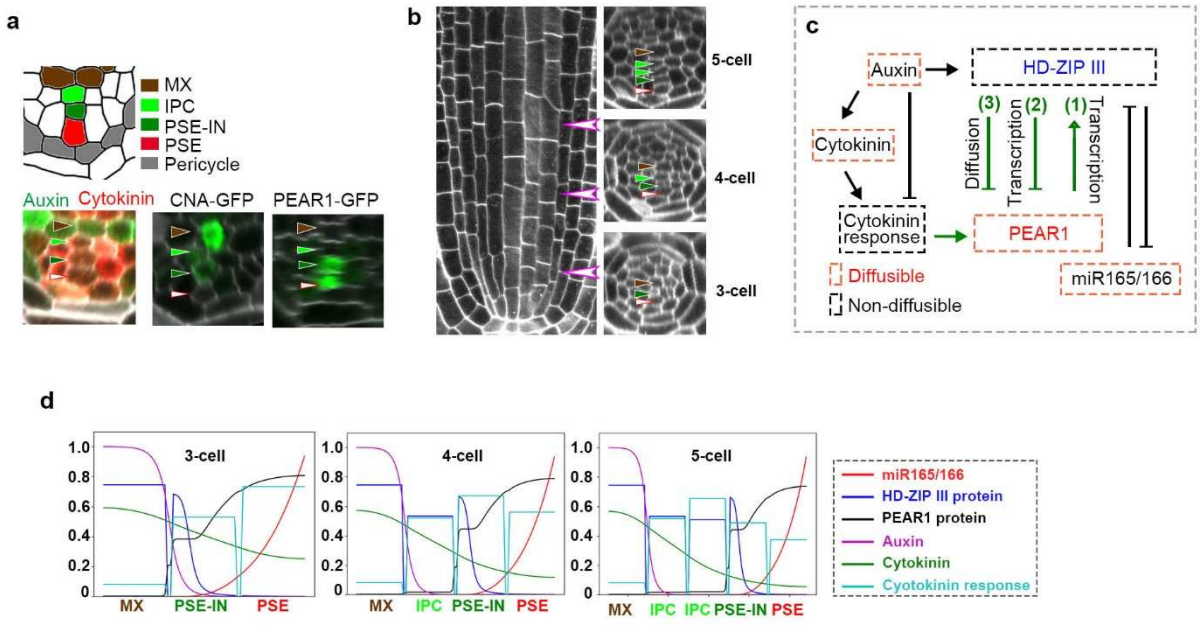

Extended Data Fig. 10| The boundary between HD-ZIP III and PEAR proteins forms within the PSE-IN.

a, Pattern of auxin, cytokinin, HD-ZIP III (CNA) and PEAR (PEAR1) in procambium. In the simulation, we simulate the concentration of HD-ZIP III and PEAR1 along the axis between metaxylem (MX, brown arrowheads) and PSE (white arrowheads). **b,** Number of cells between metaxylem and PSE increases during procambial development. Therefore, the model is defined as a line in one spatial dimension representing 3, 4 or 5 cells from the center of the xylem axis to the outer edge of the PSE cell. **c,** The regulatory network embedded within each cell. Regulatory interactions shown using a black line have been published previously, whilst those using a green line are described for the first time here. **d,** Predicted concentration gradient of all elements in 3, 4 or 5 cells (from left to right). In Figures 4p-r, only PEAR and HD-ZIP concentrations are shown, whilst all model components are shown here in all cases. Within different root geometries corresponding to different growth stages in Arabidopsis, both PEAR1 and HD-ZIP III are co-localized in PSE-IN, forming a sharp concentration boundary within this cell.